Karlsruhe Institute of Technology

Evaluated data files for n+ ^{180}W and ^{183}W irradiation at incident neutron energies up to 200 MeV

by A.Yu. Konobeyev, U. Fischer, P.E. Pereslavtsev, S.P. Simakov

KIT SCIENTIFIC WORKING PAPERS 123

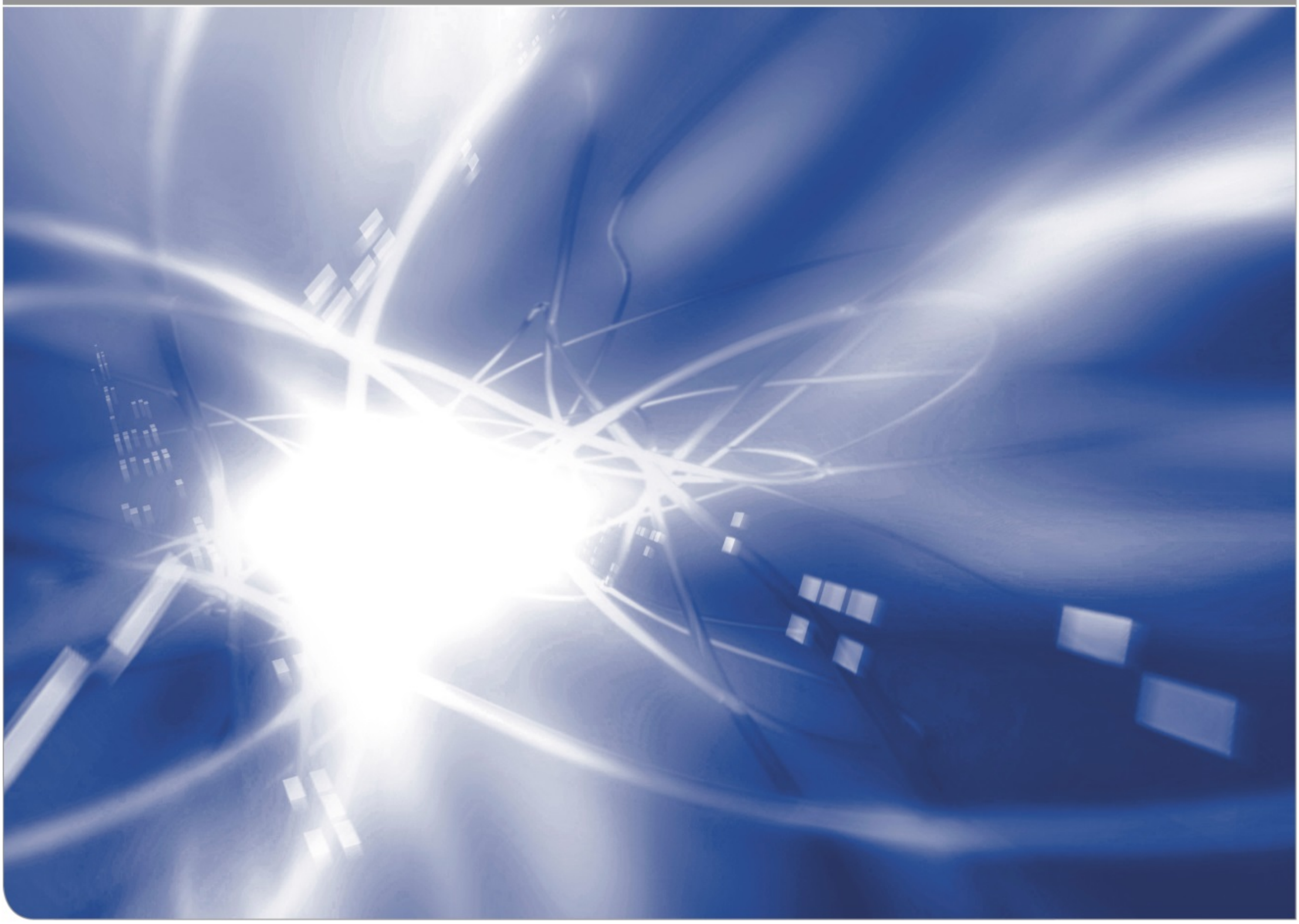

Institute for Neutron Physics and Reactor Technology, KIT

Impressum

Karlsruher Institut für Technologie (KIT)
www.kit.edu

2019

ISSN: 2194-1629

KIT Scientific Working Papers
ISSN 2194-1629
www.kit.edu

Abstract

New evaluation of nuclear data was performed for tungsten isotopes ^{180}W and ^{183}W at incident neutron energies up to 200 MeV. Calculations were carried out using a special version of the TALYS code implementing the geometry dependent hybrid model and models for the non-equilibrium light cluster emission.

The evaluation was performed using the results of calculations, available measured data, systematics predictions, and covariance information. The TEFAL code and the FOX code from the BEKED package were applied for the formatting of the data.

CONTENTS

1. INTRODUCTION

Tungsten plays a special role for the design of fusion devices and for high-energy applications. Improving the quality of data for tungsten used for neutron transport and activation calculations is an important challenging task.

The report describes evaluated data obtained for tungsten isotopes ^{180}W and ^{183}W. The present work is a continuation of the evaluation of nuclear data for tungsten isotopes [1].

The evaluation procedure concerning nuclear model calculations and the use of experimental data and systematics is described briefly in Section 2. Section 3 discusses the data evaluation for ^{180}W and Section 4 for ^{183}W.

2. BRIEF DESCRIPTION OF EVALUATION PROCEDURE

The procedure consists of theoretical calculation of cross-sections, energy and angular distributions for emitted particles and the combination of obtained data with experimental values. Final data are recorded in the ENDF-6 format.

Details are described in Ref.[1].

2.1 Nuclear model calculations

The TALYS code [2,3] with implemented geometry dependent hybrid model [4] and models for the non-equilibrium cluster emission [5,6] was applied for calculations. Details and comprehensive comparison with experimental can be found in Refs.[3,5]. The brief discussion is presented in Ref.[1].

Optical model parameters from Ref.[7] with deformation parameters from Ref.[8] for were used for calculations for ^{180}W, Appendix I. The search of optical model parameters was performed for ^{183}W to provide the best agreement with calculated angular distributions and available experimental data. Obtained parameters were used for further calculations.

The Monte Carlo method proposed in Ref.[9] was applied for the calculation of covariance matrices for cross-sections [1,10].

2.2 Processing of calculated data

Recording of preliminary data file in the ENDF-6 format was performed using the TEFAL-1.9 code [11,12]. To avoid gaps in the hard part of neutron spectra the *subroutine processchannels* of the code was slightly modified. Details are given in Appendix II.

2.3 Use of experimental data

Experimental data from Refs.[13-58] were used for the preparation of evaluated data for ^{180}W and ^{183}W. The citations are based on EXFOR records [59]. In some cases, errors of measured data were updated or specified using available information.

2.4 Use of systematics

Total cross-sections measured in Ref.[25] for ^{182}W, ^{184}W, and ^{186}W were used to estimate the total reaction cross-section for isotopes ^{180}W and ^{183}W. The estimation was made applying the method of the calculation [60] basing on the parameterization of a large number of experimental data. The method [60] is also used in the CEM and MCNP6 codes [61].

Total cross-sections for ^{180}W and ^{183}W were estimated as follows

$$\sigma^{(x)}_{tot} = (1/3)\ \sigma^{(x)}_{tot,B} \left(\sigma^{(182)}_{tot,D} \big/ \sigma^{(182)}_{tot,B} + \sigma^{(184)}_{tot,D} \big/ \sigma^{(184)}_{tot,B} + \sigma^{(186)}_{tot,D} \big/ \sigma^{(186)}_{tot,B} \right) , \qquad (1)$$

where the upper index relates to the mass number of tungsten isotope; “x” is equal to 180 or 183; the lower index “B” indicates the cross-section calculated using the parameterization from Ref.[60] and “D” relates to the measured data [25].

Obtained data are shown in figures below as “*based on Dietrich (03)*”.

The data from Ref.[62] were applied for the correction of calculated total light particle production cross-sections. Data [62] were obtained as a result of the evaluation of the atomic mass number dependency of corresponding cross sections at fixed neutron incident energy, by analogy with the usual evaluation of the energy dependence of reaction cross sections for a fixed nucleus. See details in Refs.[62,63]. Data [62] are plotted in figures below as “*reference data*”.

2.5 Cross-section evaluation

The combination of experimental data and results of model calculations was performed using the covariance information and the generalized least-squares method (GLS). The code from Ref.[64] was applied for numerical calculations.

2.6 Recording data in ENDF-6 format

Data obtained were consistently integrated in the final data file using the FOX code from the BEKED package [10]. More details can be found in Ref.[1].

Obtained data file was tested using codes from Ref.[65] and the COVEIG code [66] and processed using the NJOY [67] code.

3. DATA OBTAINED FOR ^{180}W

The Section describes the evaluated data for ^{180}W and presents the comparison with data from different libraries, measured data, systematics, and calculations.

Cross-sections, energy and angular distributions from following evaluated data libraries are plotted in figures below, if appropriate: EAF-2010 [68], JENDL-4.0 [69], JENDL-4/HE [70], JENDL/AD-2017 [71], JENDL-HE [72], ENDF/B-VIII [8], TENDL-2017 [11,73], and JEFF-3.3 [74].

3.1 Resonance parameters

Resonance parameters were taken from the Mughabghab compilation [75]. The upper energy limit for the resonance region is equal to 100 eV.

3.2 Total cross-section

Figures 1 and 2 show the total cross-section for ^{180}W obtained in this work, data from different libraries, measured data, and cross-sections derived from experimental data [25] as described in Section 2.4. For better view data from JEFF-3.3 are presented after the averaging over selected energy groups.

The cross sections obtained are close to the JENDL-4 and ENDF/B-VIII data at energies up to 20 MeV and to data estimated using measurements in Ref.[25] at higher energies. Some differences are observed with the data from JEFF-3.3 and TENDL-2017.

The JEFF-3.2 file for ^{180}W is part of the TENDL-2015 library [76].

3.3 Elastic and inelastic scattering cross-section

The elastic cross-section is plotted in Fig.3. As in the case of total cross-section, the difference with JEFF-3.3 and TENDL-2017 data is observed mainly at energies from 0.02 to 2 MeV.

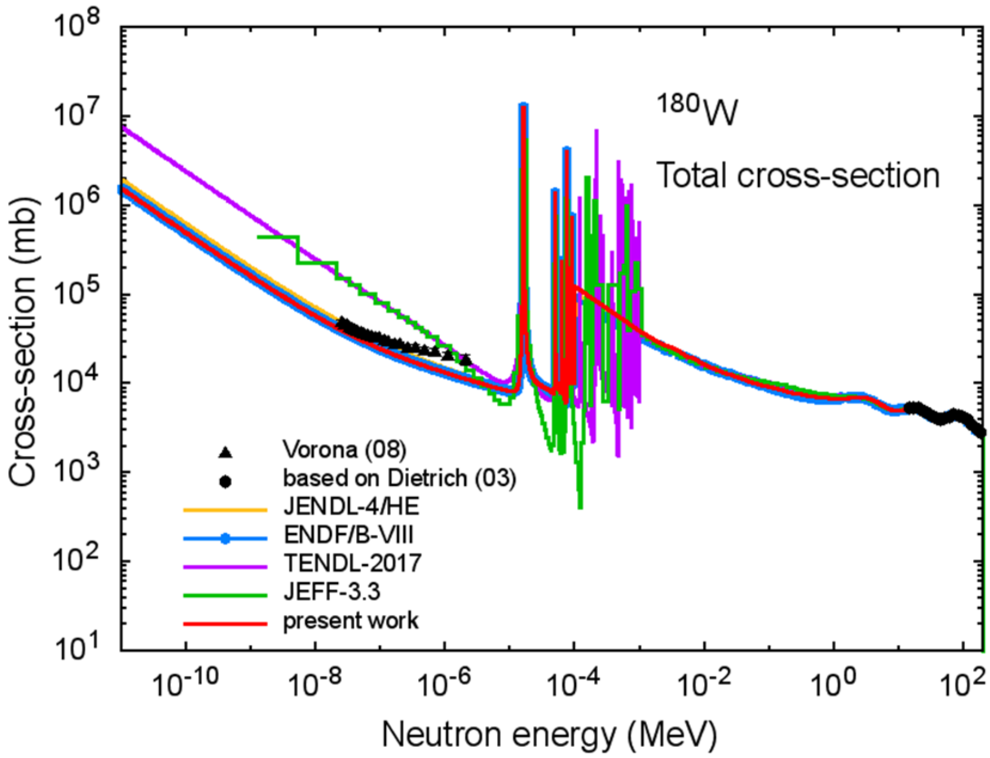

Fig.1 Total cross-section for ^{180}W at neutron incident energies from 10^{-11} to 200 MeV obtained in the present work, measured data, cross-section derived using experimental data for tungsten isotopes $^{182,184,186}W$ ("*based on Dietrich (03)*"), and data taken from different libraries. See explanations in the text.

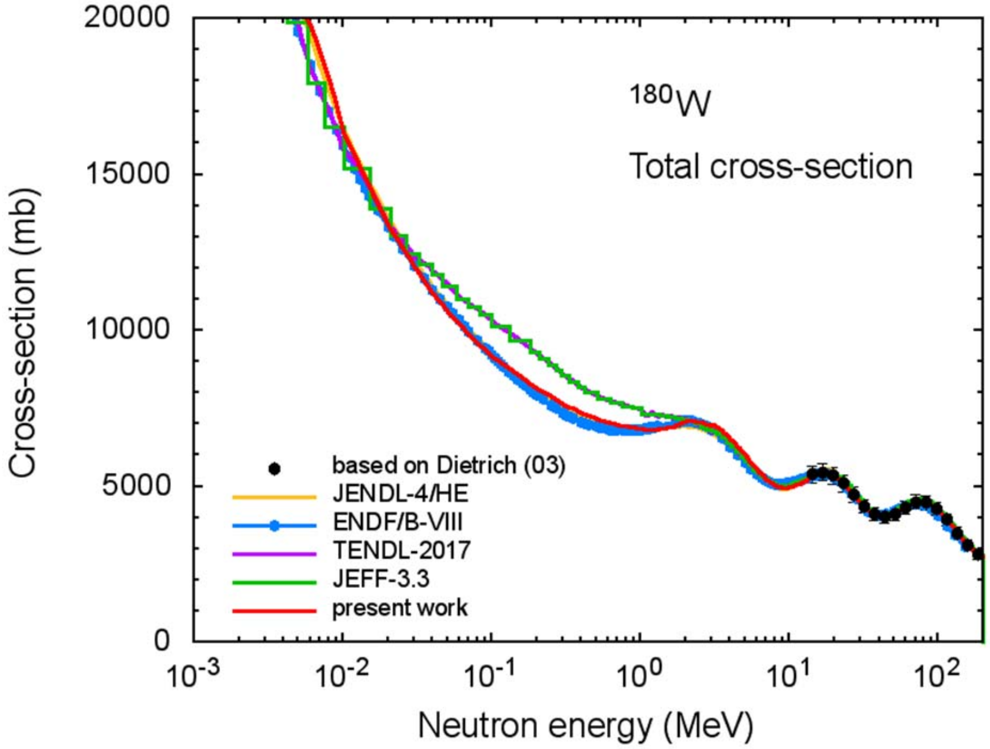

Fig.2 Total reaction cross-section for neutron irradiation of ^{180}W at neutron incident energies from 0.001 to 200 MeV. See comments to Fig.1

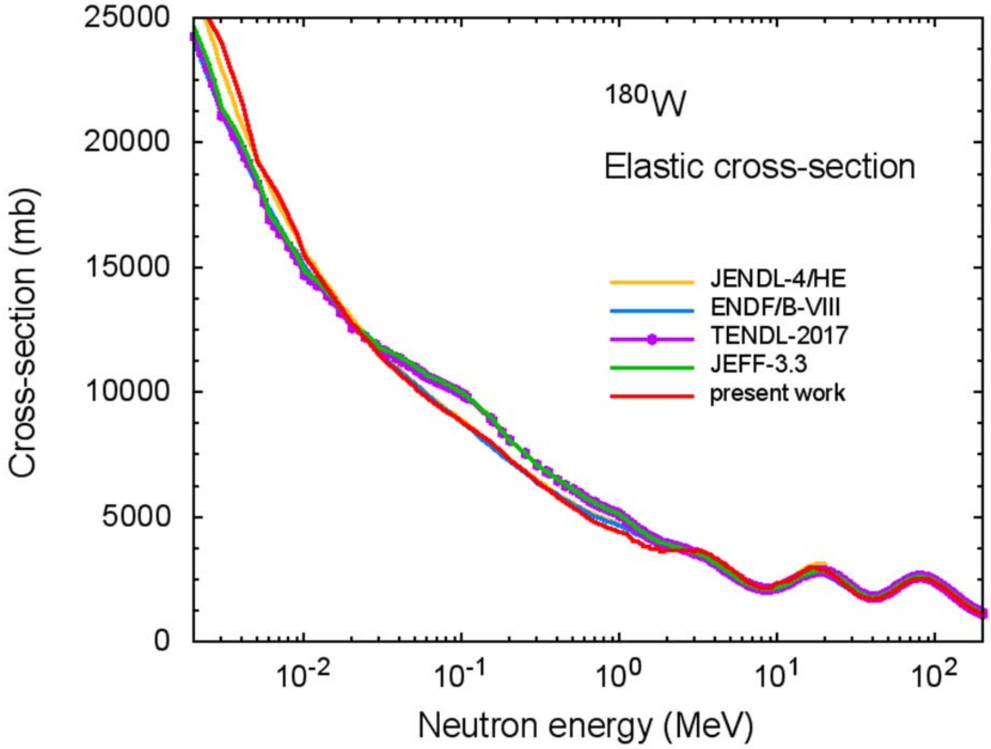

Fig.3 Cross-section for elastic neutron scattering for ^{180}W evaluated in the present work, measured data, and data taken from different libraries.

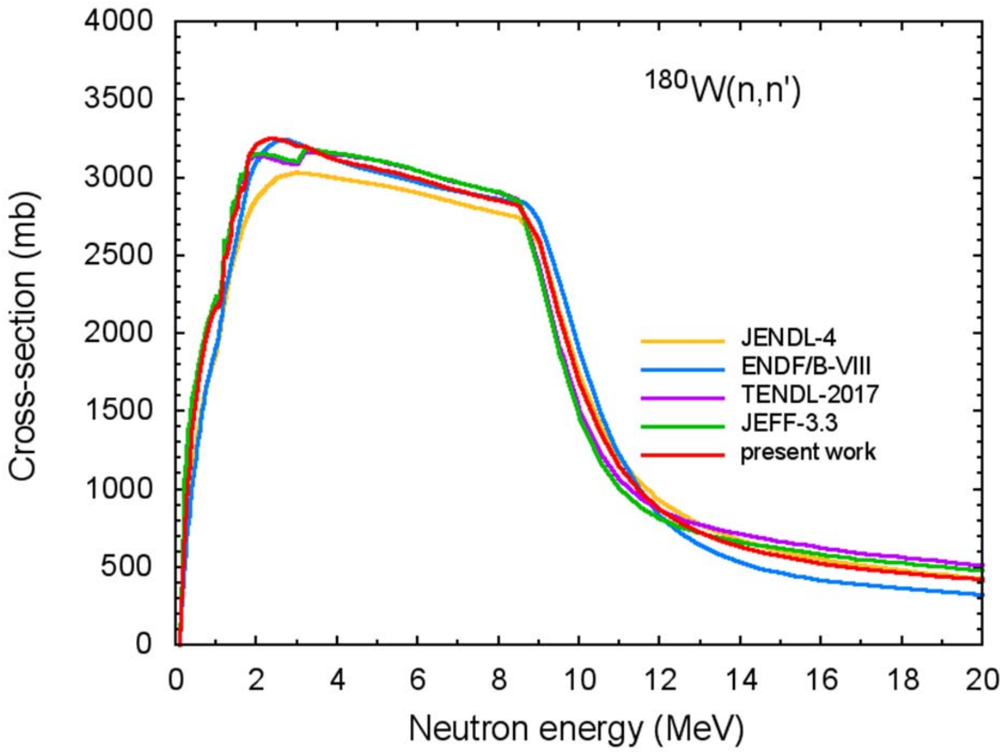

Fig.4 Inelastic scattering cross-section $^{180}W(n,n')$.

Figure 4 show the neutron inelastic scattering cross-section (n,n’). The cross-section obtained and data from different libraries are relatively close.

3.4 Cross-sections for various reactions

Figures 5-10 show cross-sections evaluated for different nuclear reactions. In general, new data are in good agreement with experimental data.

As for other tungsten isotopes [1] the difference between evaluated (n,γ) reaction cross-section and data from other libraries is observed at neutron energies, where experimental data are not available (Fig.5).

The evaluated (n,2n) reaction cross-section with the production of residual in both ground and metastable states is close to EAF-2010 data (Fig.6). This also applies to the ^{179g}W production (Fig.7). A certain difference is observed between new cross-sections and JEFF-3.3, and TENDL-2017 at neutron energies below 17 MeV data and between ENDF/B-VIII data at energies above 11 MeV.

The obtained $^{180}W(n,2n)^{179m}W$ cross-sections are close to JENDL-4 data (Fig.8). There is agreement between different cross sections in the energy region close to the reaction threshold.

Obtained (n,p) reaction cross-section is close to the cross-section from TENDL-2017 and is somewhat different from the JENDL/AD-2017 data (Fig.9).

There is good agreement between new data and cross-sections for ^{180}W(n,p)^{180g}Ta reaction from JENDL/AD-2017 (Fig.10).

3.5 Light particle production cross-sections

Figure 11 shows the neutron production cross-section for n+^{180}W interactions and Figs.12-16 plot the proton- deuteron-, triton-, ^{3}He-, and α-particle formation cross-sections.

To illustrate the difference between evaluated cross-sections, other data, and theoretical calculations, Figs.11-16 show cross-sections from different libraries and results of calculations performed with the intranuclear cascade evaporation model implemented in the CASCADE code [77,78] and CEM03 code [79,80].

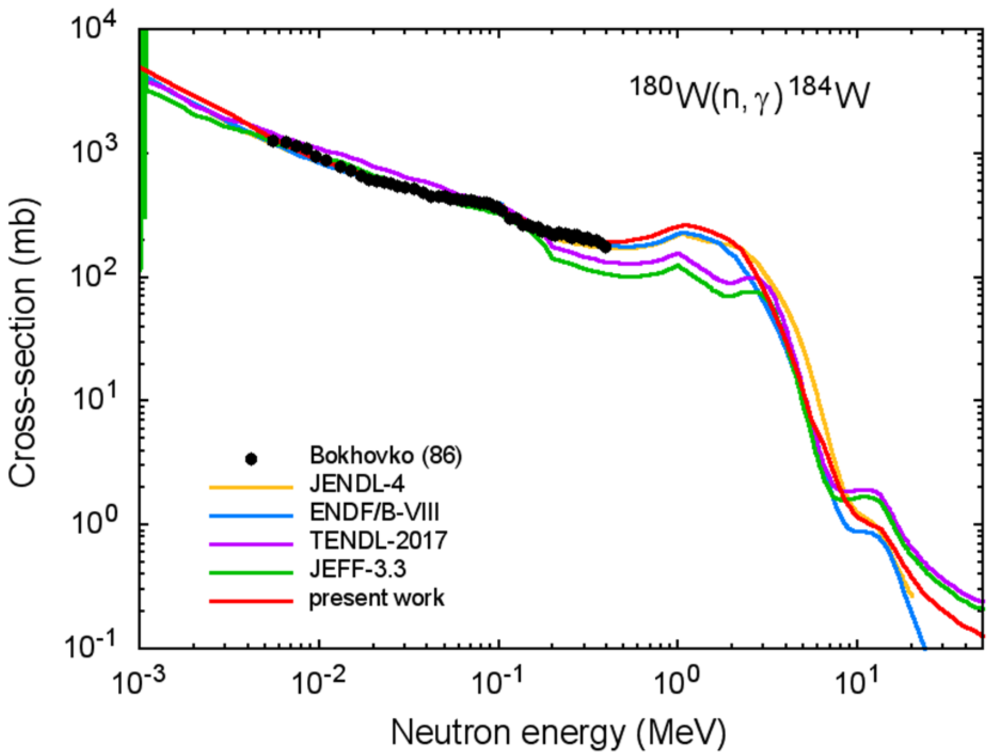

Fig.5 (n,γ) reaction cross-section for ^{180}W.

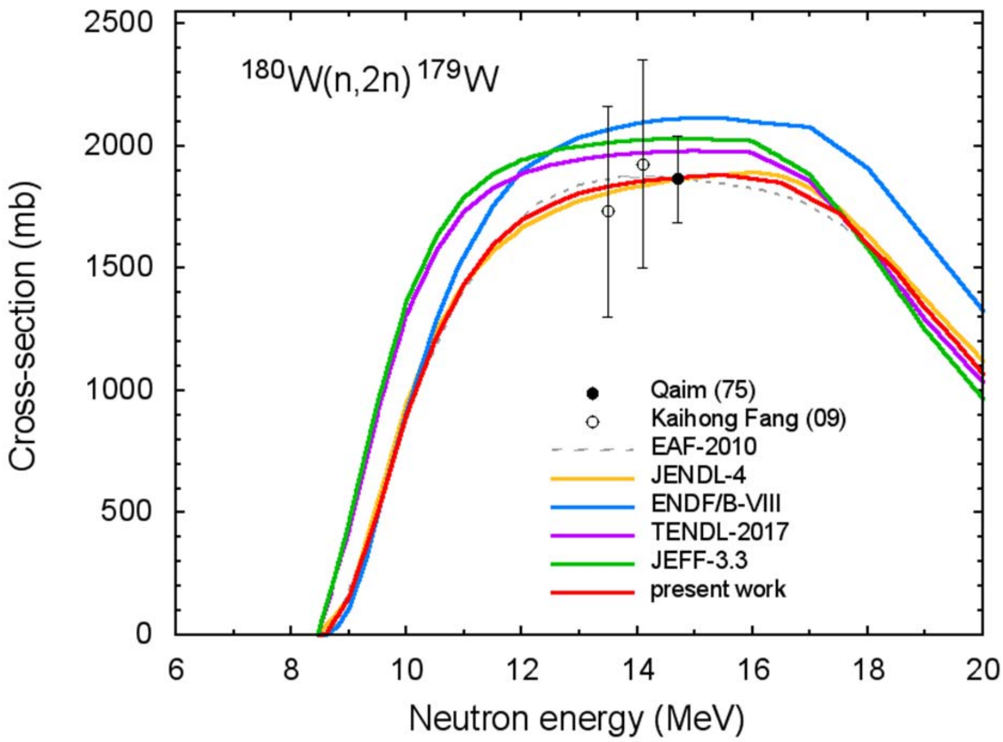

Fig.6 (n,2n) reaction cross-section for ^{180}W equal to the sum of ^{179g}W and ^{179m}W production cross-sections.

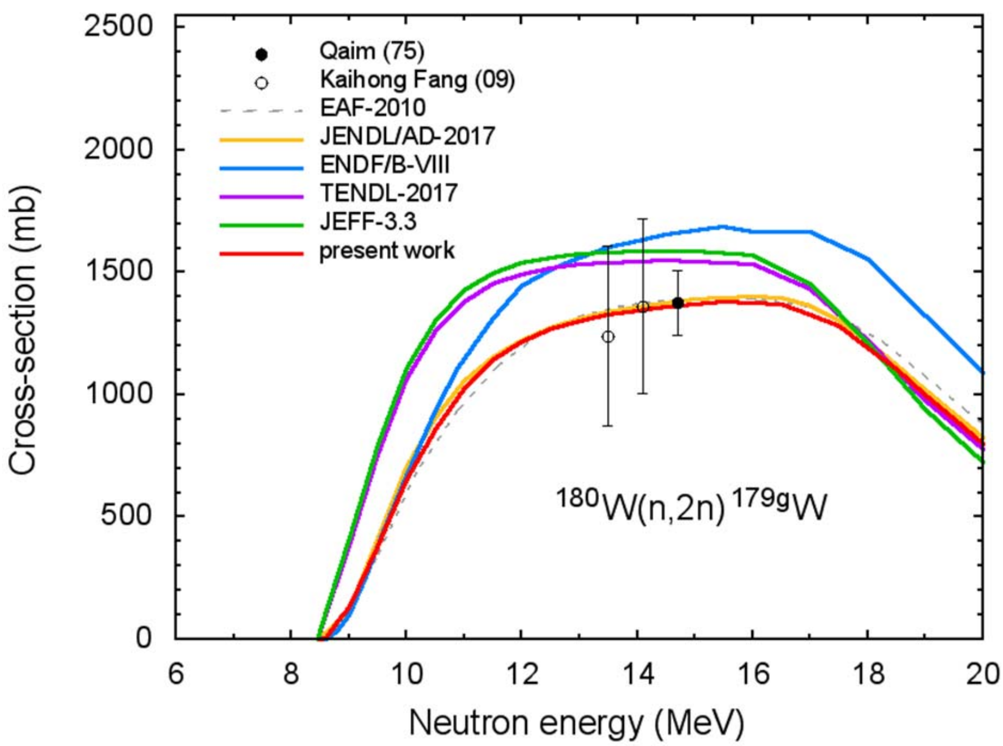

Fig.7 (n,2n) reaction cross-section for ^{180}W with the production of ^{179}W in the ground state.

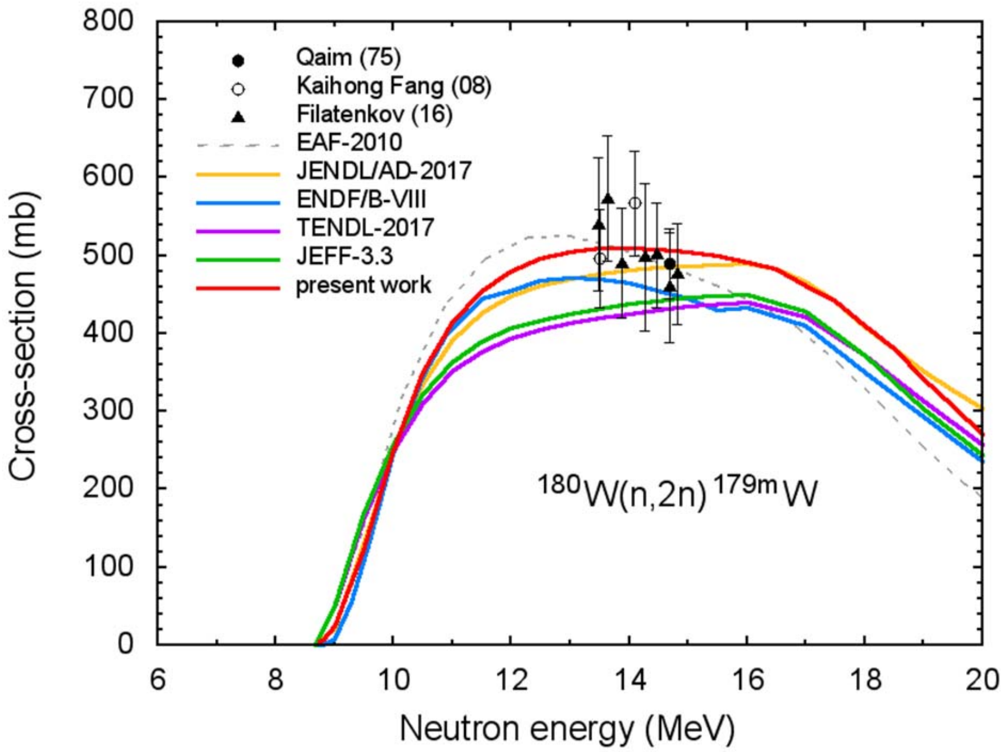

Fig.8 (n,2n) reaction cross-section for ^{180}W with the production of ^{179}W in the metastable state ($T_{1/2}$ = 6.4 m).

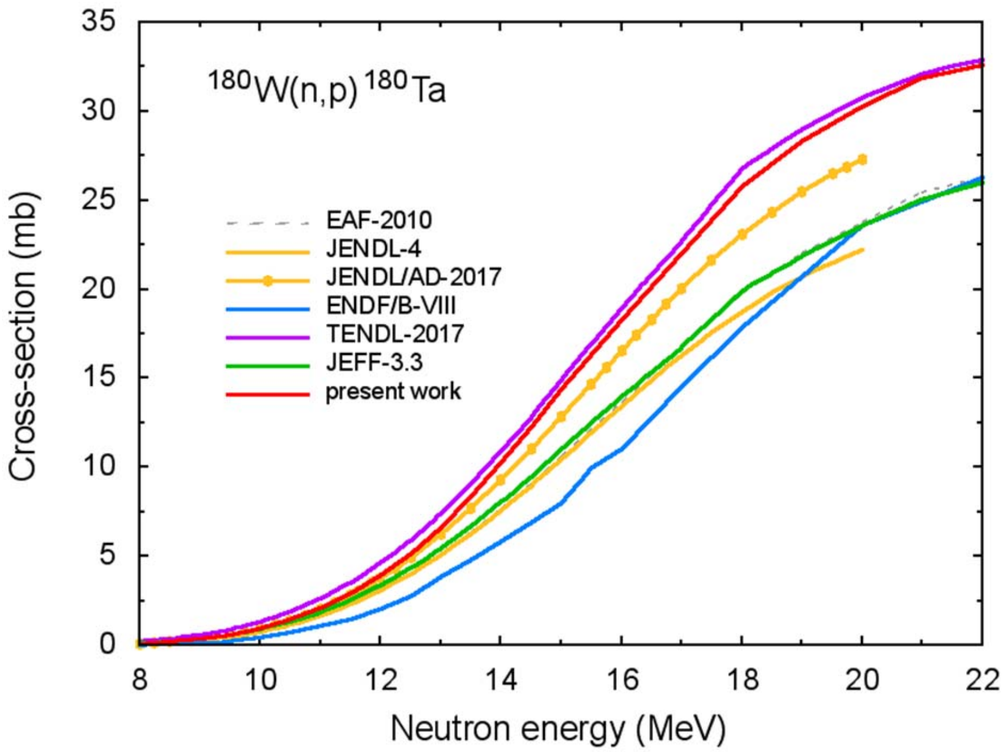

Fig.9 (n,p) reaction cross-section for ^{180}W equal to the sum of ^{180g}Ta and $^{1809m}Ta$ production cross-sections.

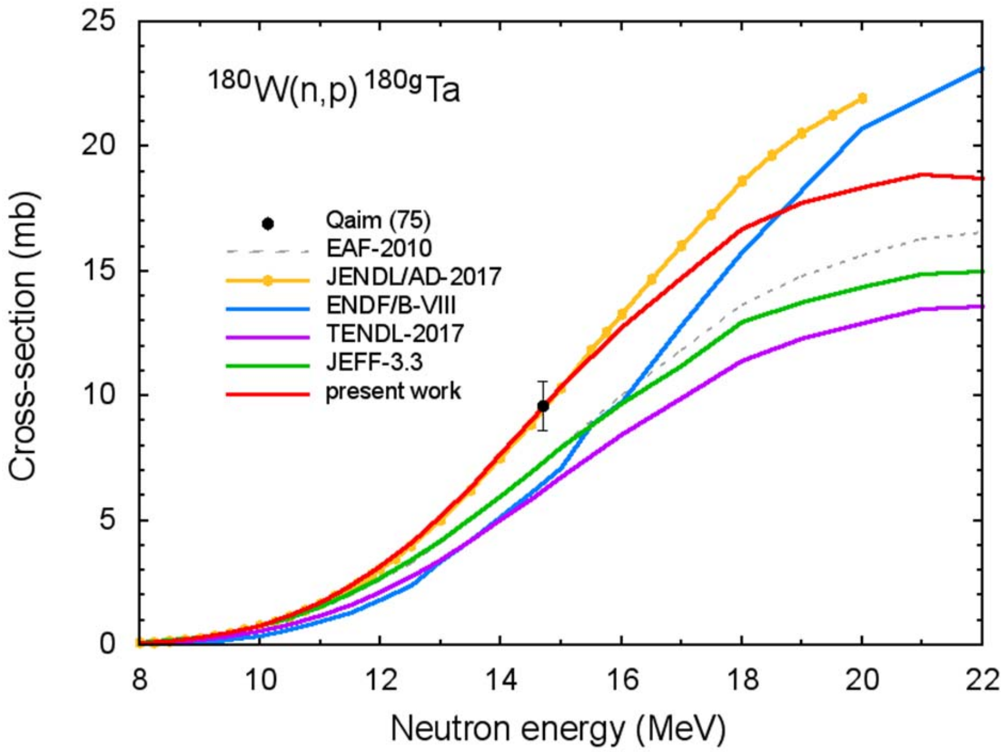

Fig.10 (n,p) reaction cross-section for ^{180}W with the production of ^{180}Ta in the ground state.

For comparison, Figs.11-16 show also the evaluated “reference” data [62], discussed in Section 2.4.

In general, the energy dependence of obtained cross sections seems reasonable, and the absolute values are consistent with the estimated data [62].

3.6 Atomic displacement cross-section

The atomic displacement cross-section (σ_d) for ^{180}W calculated using evaluated data and the NJOY code [67] is shown in Fig.17. Results of calculations with the CEM03 code are also plotted.

Cross-sections calculated using data from different libraries are in relative good agreement at neutron energies up to 100 MeV. New σ_d values are consistent with calculations performed using the CEM03 code [79,80] implementing the cascade exciton model, justified at intermediate and high energies.

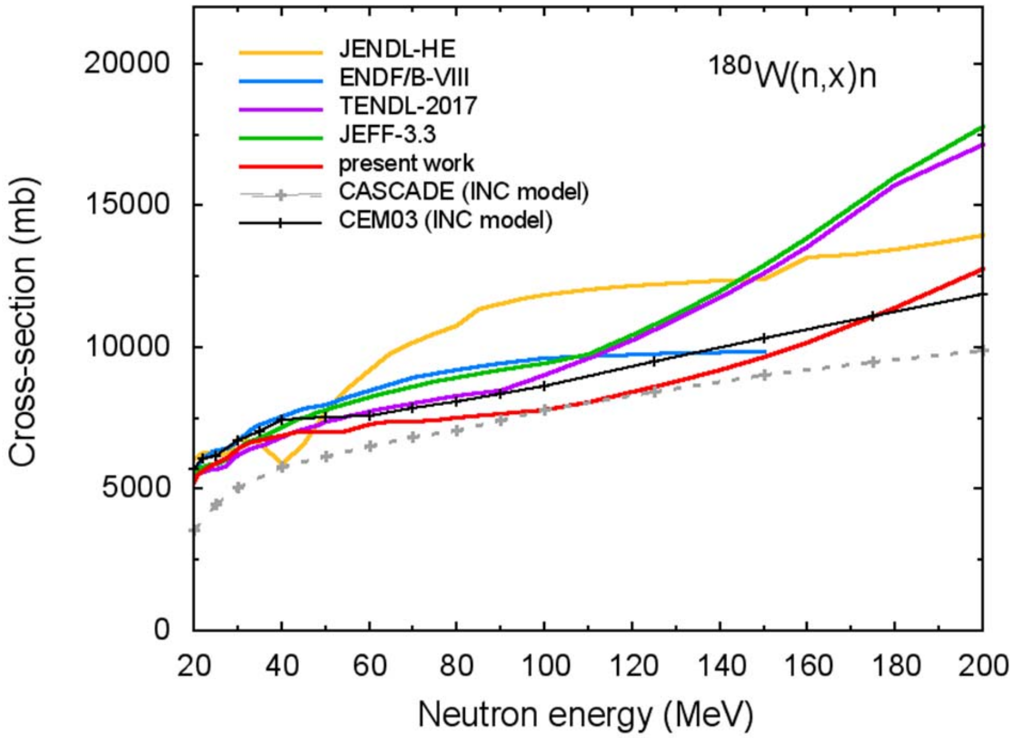

Fig.11 Neutron production cross-section for ^{180}W. See explanations in the text.

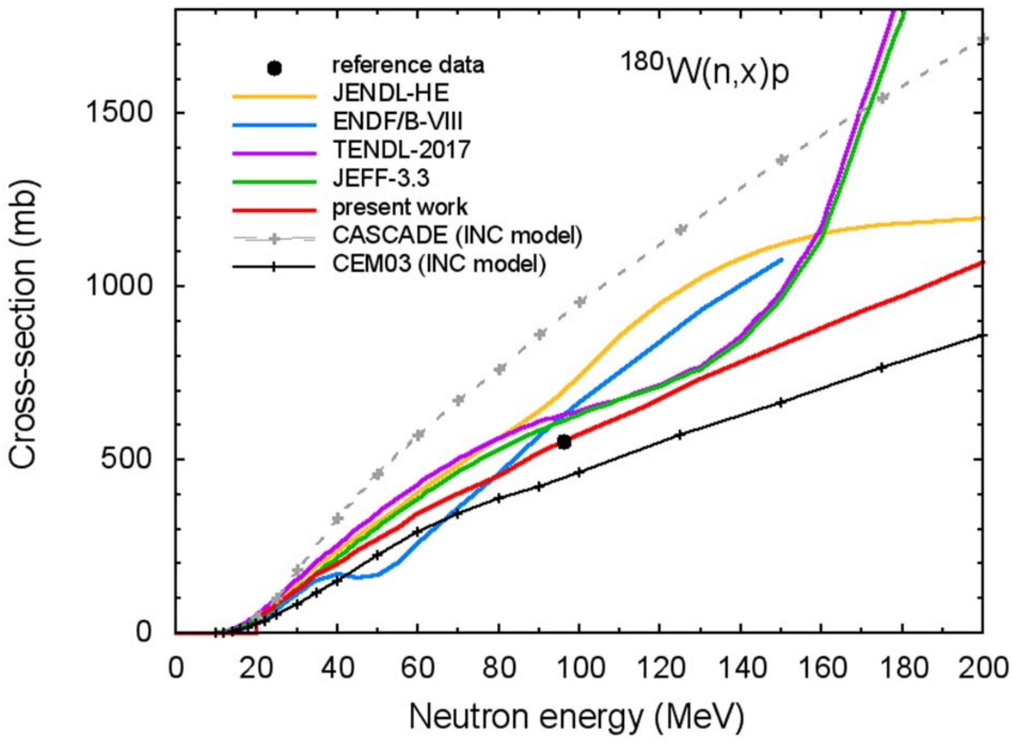

Fig.12 Proton production cross-section for ^{180}W.

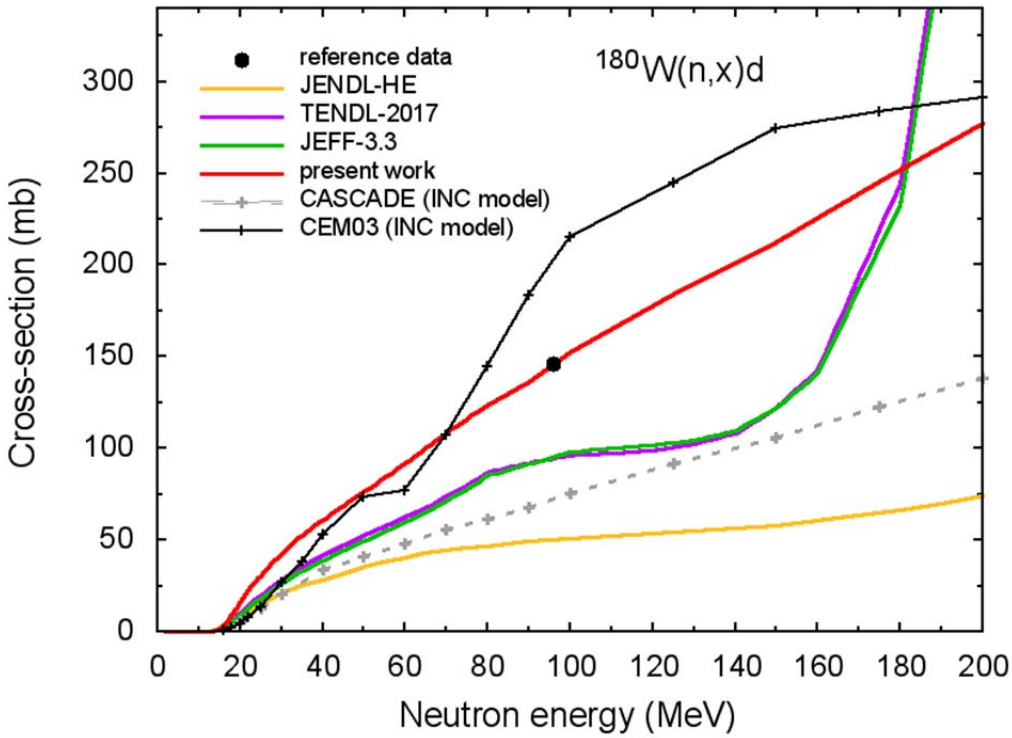

Fig.13 Deuteron production cross-section for ^{180}W.

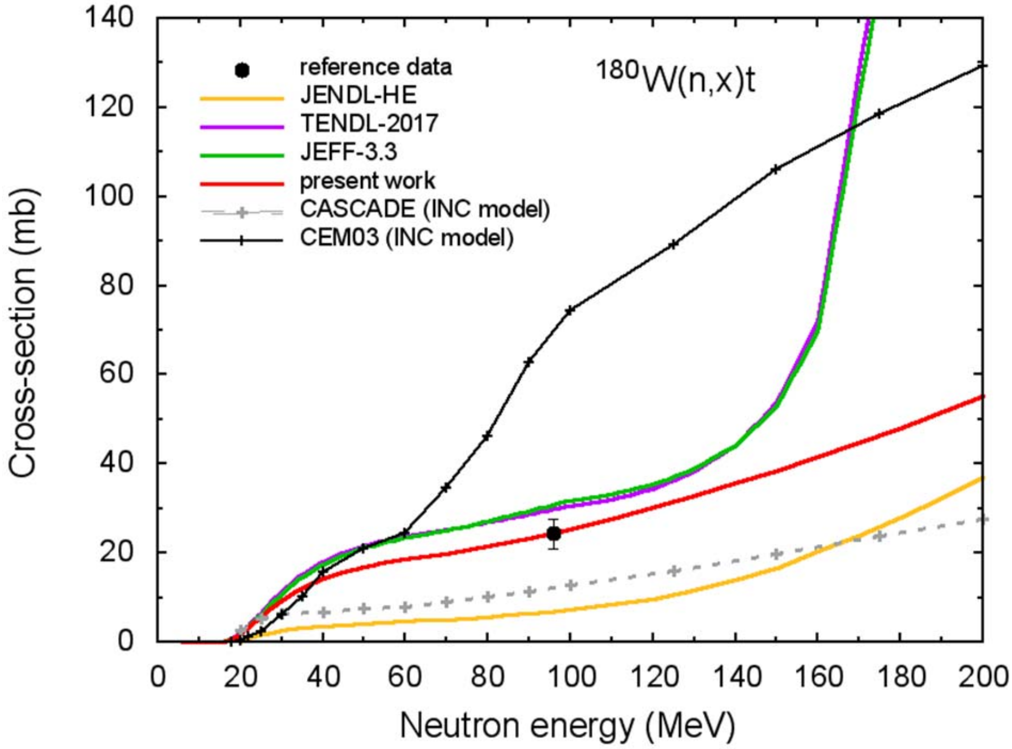

Fig.14 Triton production cross-section for ^{180}W.

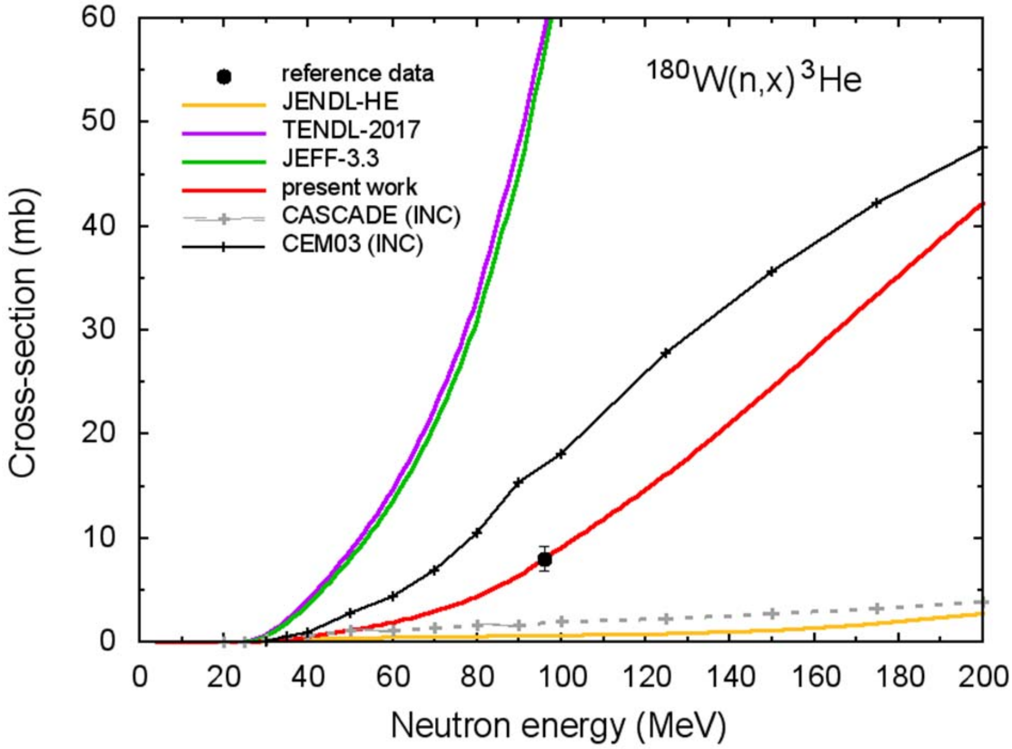

Fig.15 ^{3}He production cross-section for ^{180}W.

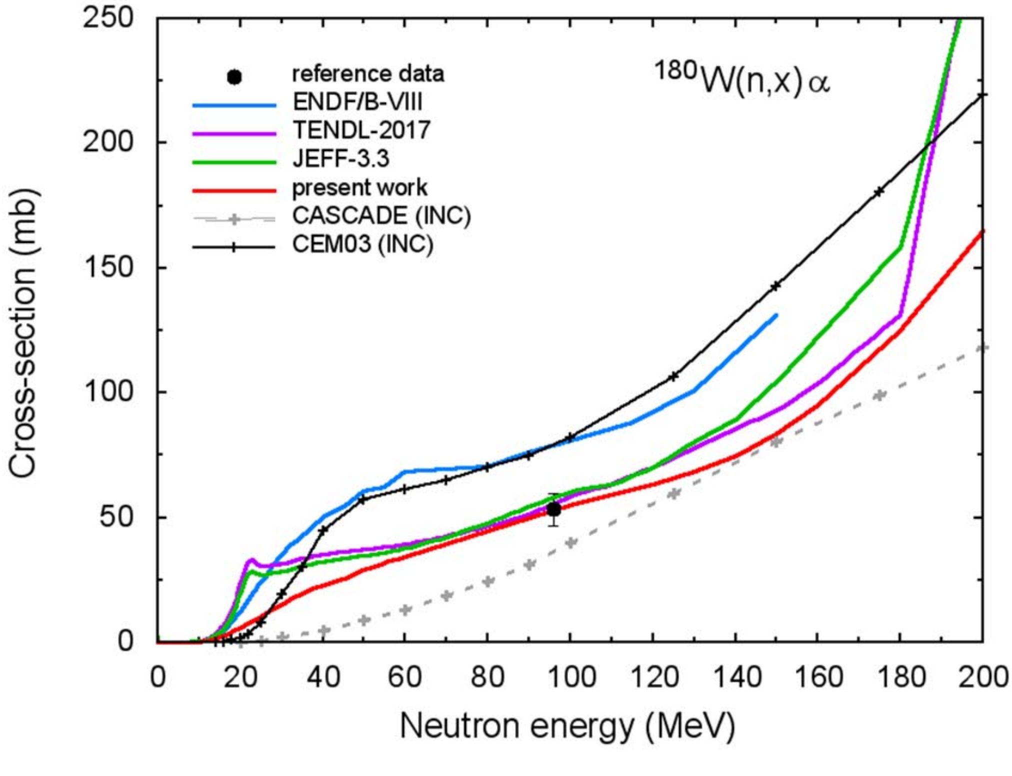

Fig.16 α-particle production cross-section for ^{180}W.

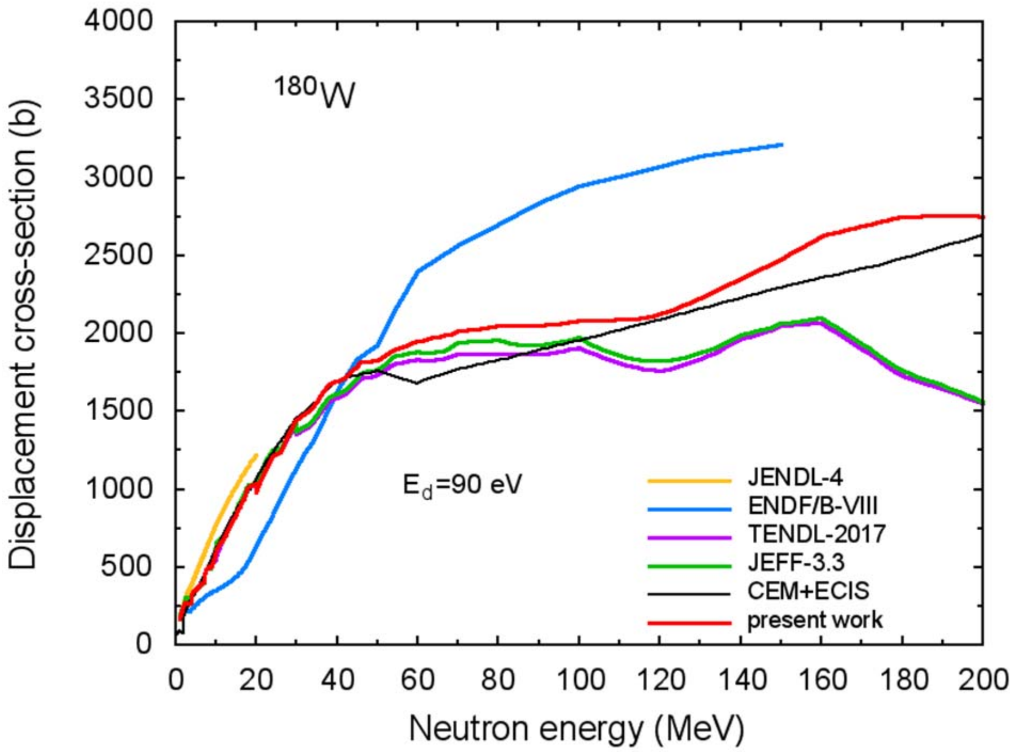

Fig.17 Atomic displacement cross-section for ^{180}W.

4. DATA OBTAINED FOR ^{183}W

4.1 Total cross-section

Figures 18 and 19 show evaluated total cross-section, data from different libraries, experimental data, and cross-sections derived using measurements [25] for other tungsten isotopes.

Obtained data are in good agreement with available experimental information.

4.2 Cross-section and angular distributions for elastic scattering

The elastic scattering cross-section is plotted in Fig.20. Evaluated cross-sections are close to ENDF/B-VIII data at energies up to 12 MeV and to JEFF-3.3 and TENDL-2017 data at higher neutron energies.

The elastic scattering angular distributions ($d\sigma/d\Omega$) are shown in Figs.21-26.

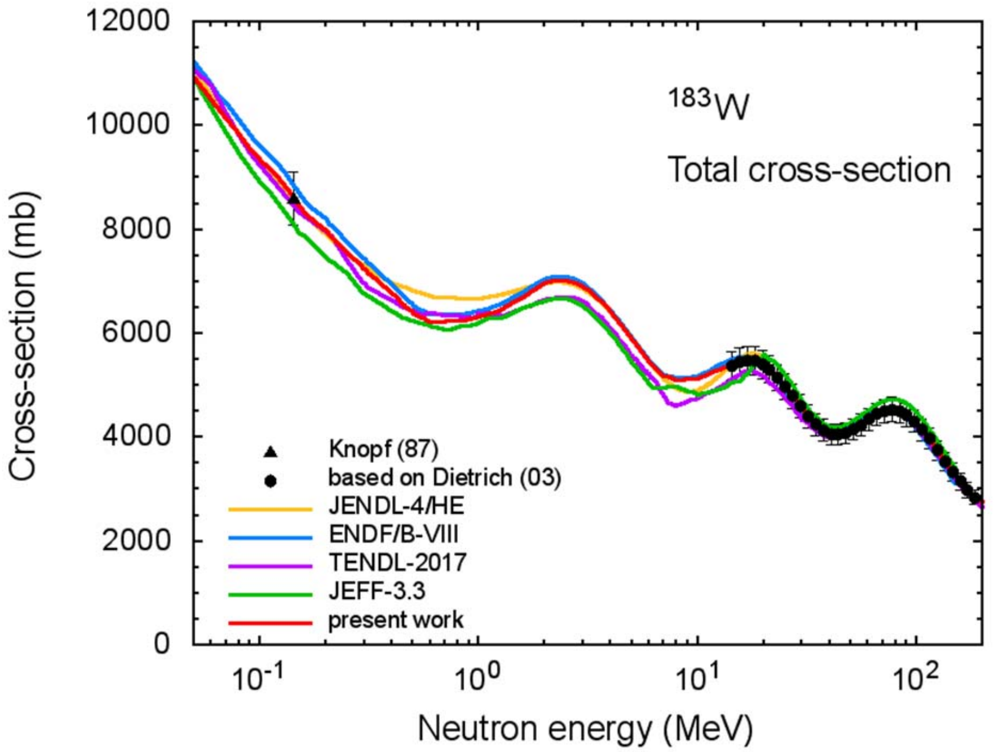

Fig.18 Total reaction cross-section for neutron irradiation of ^{183}W evaluated in the present work, measured data, cross-section derived using experimental data for tungsten isotopes ^{182,184,186}W ("*based on Dietrich (03)*"), and data taken from different libraries. See explanations in the text.

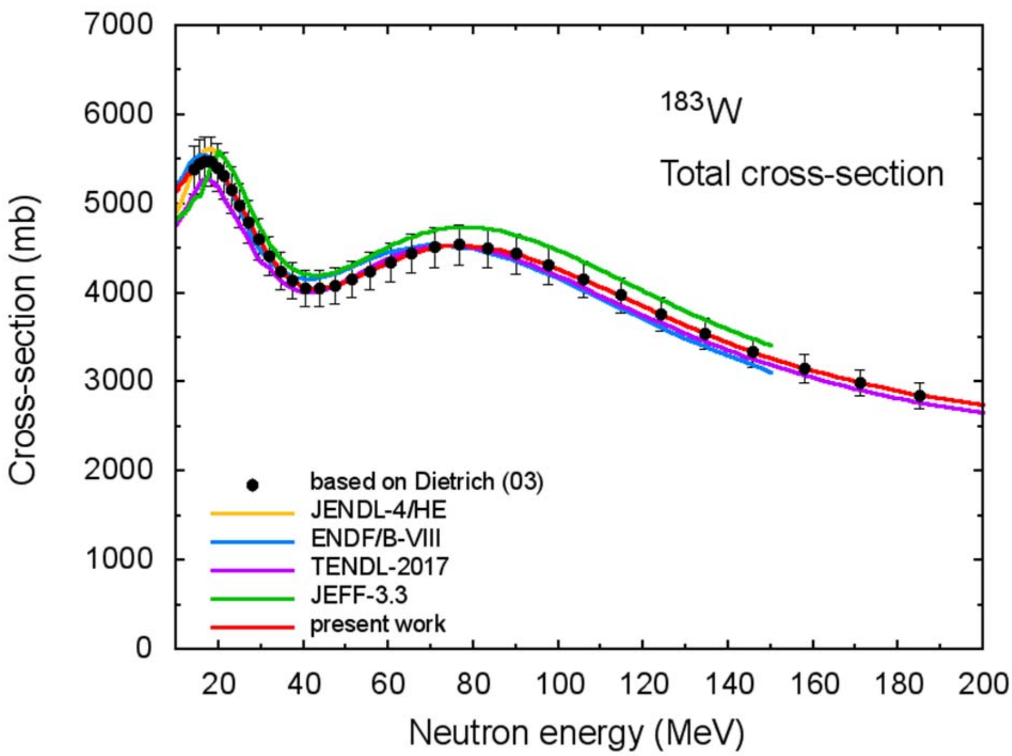

Fig.19 The same as in Fig.18 at neutron incident energies from 10 to 200 MeV.

There is relative good agreement between obtained $d\sigma/d\Omega$ values and measured data. Of course, the agreement is, to some extent, conditional, since the measurements, with the exception of [23], Fig.23, were performed for the natural mixture of isotopes and experimental energies do not always coincide with the calculation energies.

4.3 Inelastic scattering cross-section

Inelastic neutron scattering cross-section is shown in Fig.27. Various data are in relative agreement.

The component of $^{183}W(n,n')^{183m}W$ reaction cross-section with the production of ^{183}W in the metastable state is shown in Fig.28. Data, with the exception of EAF-2010, agree well at energies up to 6 MeV. Obtained cross-sections are consistent with the measurements [13] and differ from other evaluations at energies above 8 MeV. Present data reflect the contents of the obtained data file dated April 2019 [81] and are preliminary in nature. It cannot be ruled out that they will be changed in the future.

4.4 Cross-sections for various reactions

Cross-sections for reactions, for which measured data are available, are plotted In Figs. 29-34.

There is two types of evaluated data for the (n,p) reaction, JENDL-4, JEFF-3.3, and TENL-2017 data are close to measurements [52], Fig.31, and ENDF/B-VIII data to ones from Ref.[27]. The evaluated cross sections in this work were obtained using all experimental data, except [42], without any preferences, and calculated cross sections, after applying the GLS method.

In general, data obtained are consistent with measured data.

The scatter of the (n,p) and (n,α) reaction cross sections, Figs.31-33, evaluated by various authors, in the energy region, where there are no experimental data, reflects the uncertainty of predictions of modern calculation models.

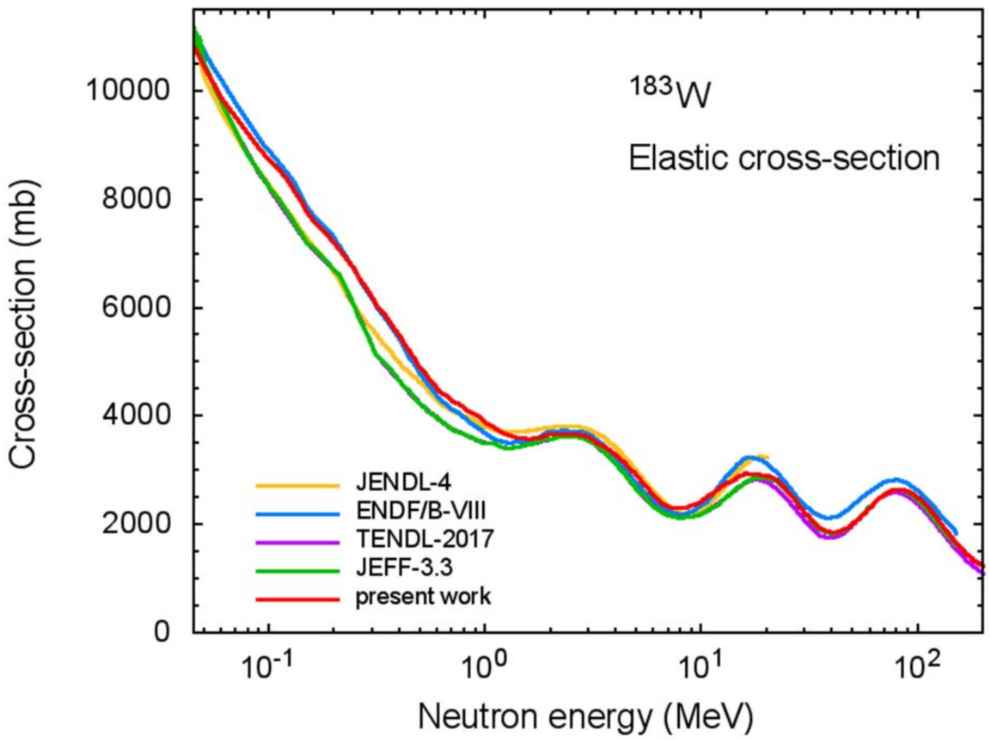

Fig.20 Elastic cross-section for neutron irradiation of ^{183}W.

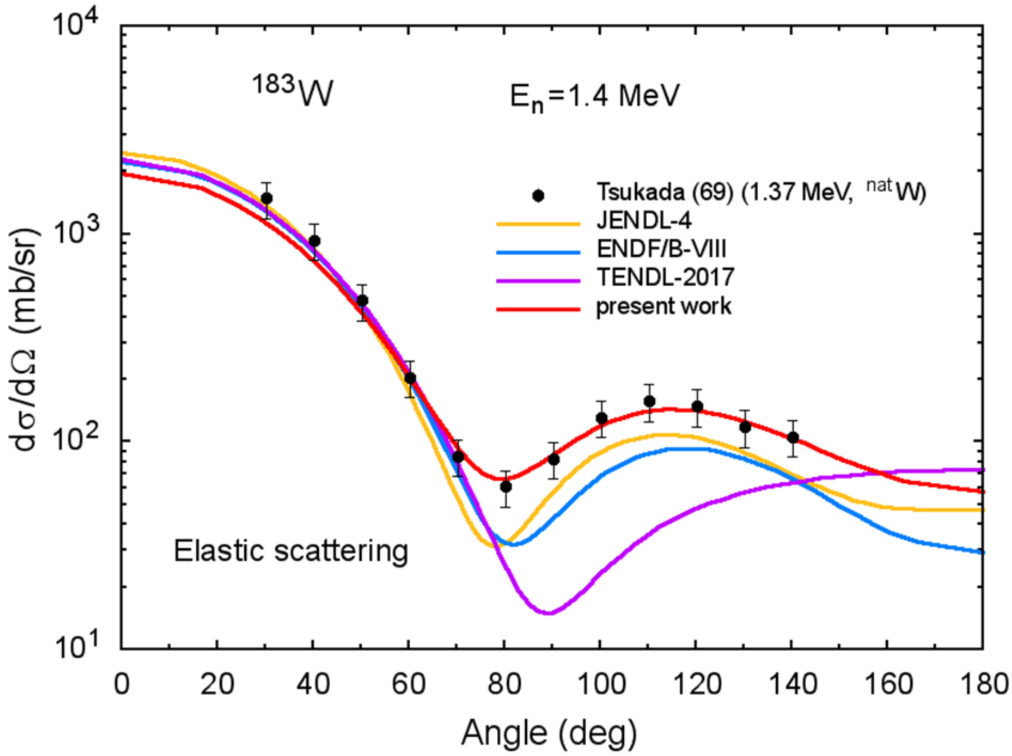

Fig.21 Elastic scattering angular distribution of neutrons for ^{183}W irradiated with 1.4 MeV neutrons.

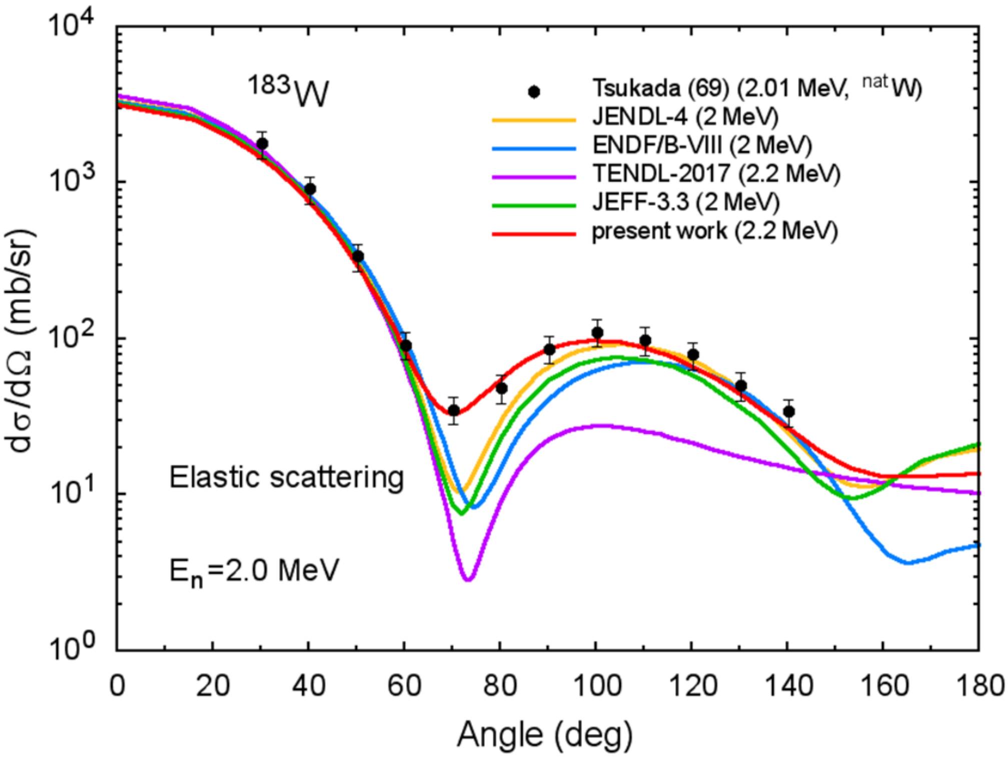

Fig.22 Elastic scattering angular distribution of neutrons for ^{183}W irradiated with 2.0 MeV neutrons.

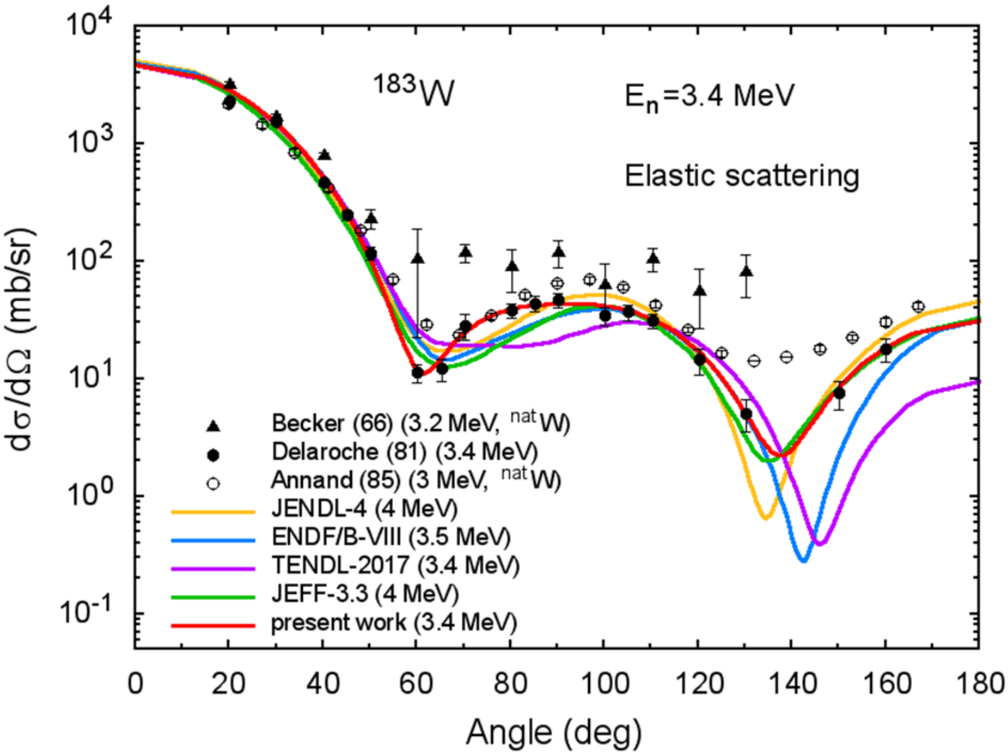

Fig.23 Elastic scattering angular distribution of neutrons for ^{183}W irradiated with 3.4 MeV neutrons.

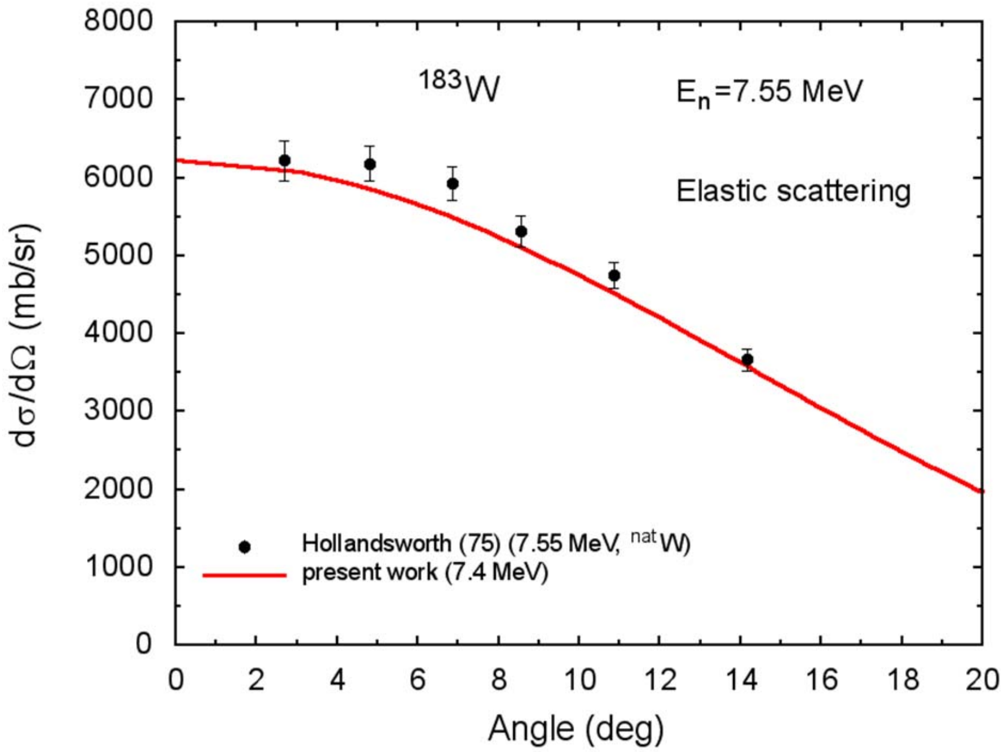

Fig.24 Elastic scattering angular distribution of neutrons for ^{183}W irradiated with 7.55 MeV neutrons.

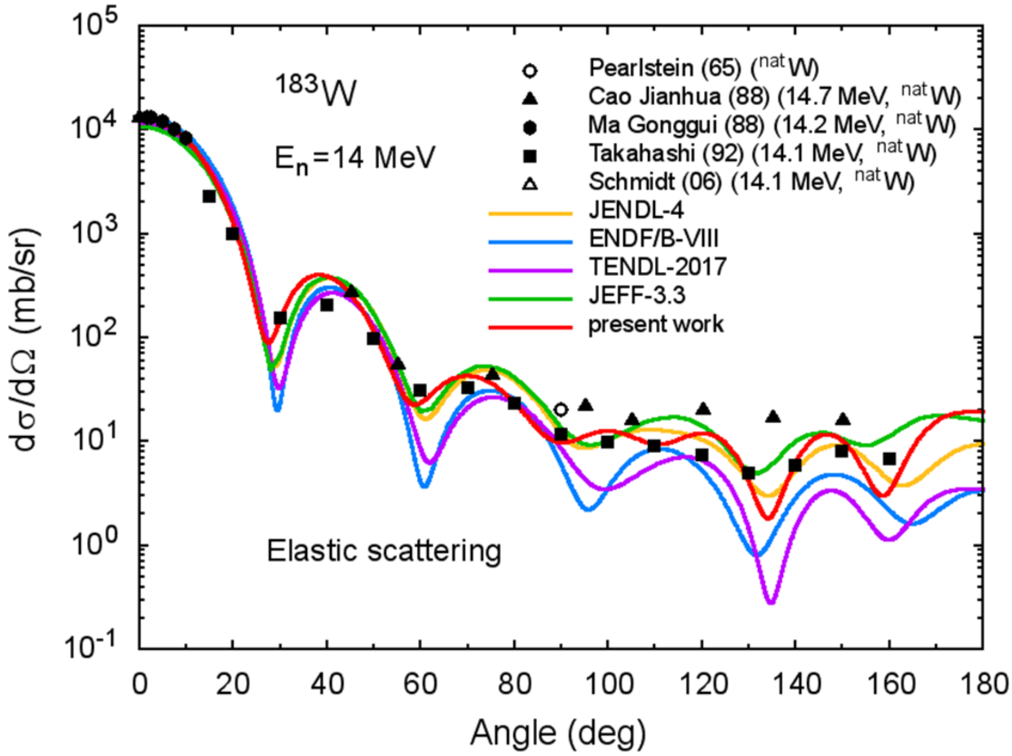

Fig.25 Elastic scattering angular distribution of neutrons for ^{183}W irradiated with 14 MeV neutrons.

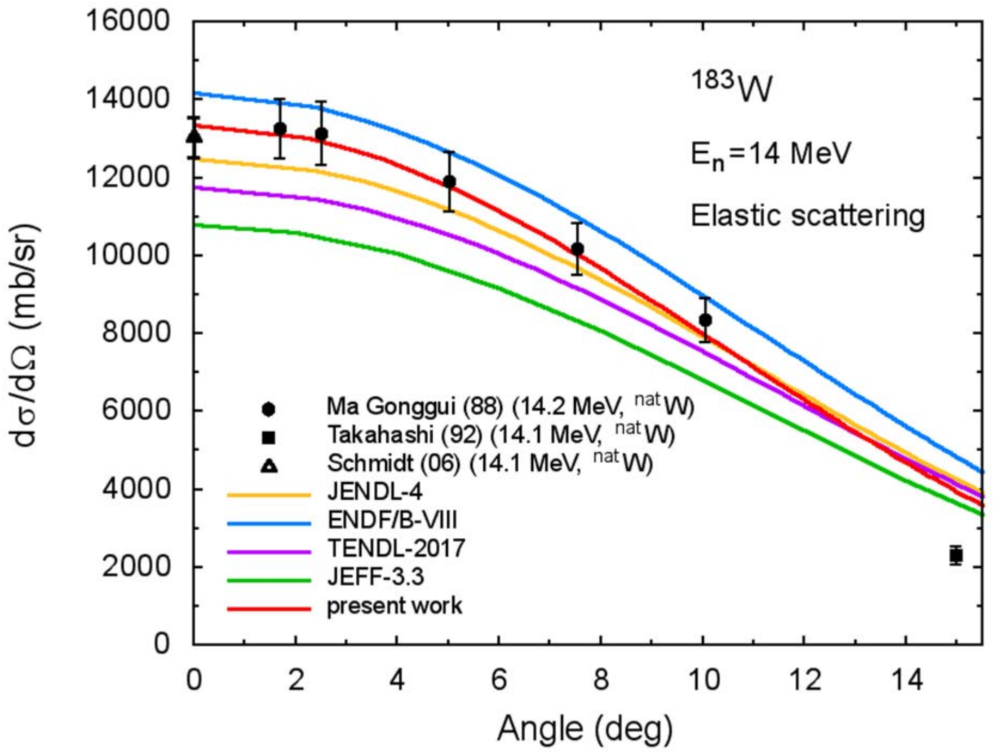

Fig.26 The same as in Fig.24 for small scattering angles.

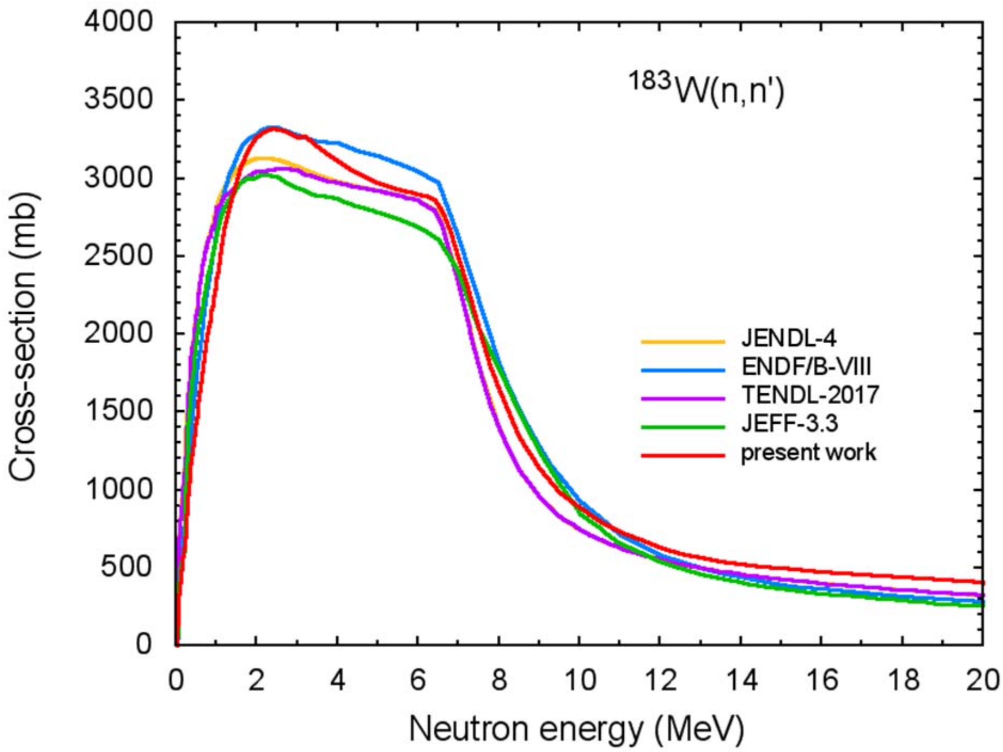

Fig.27 Inelastic scattering cross-section ^{183}W(n,n').

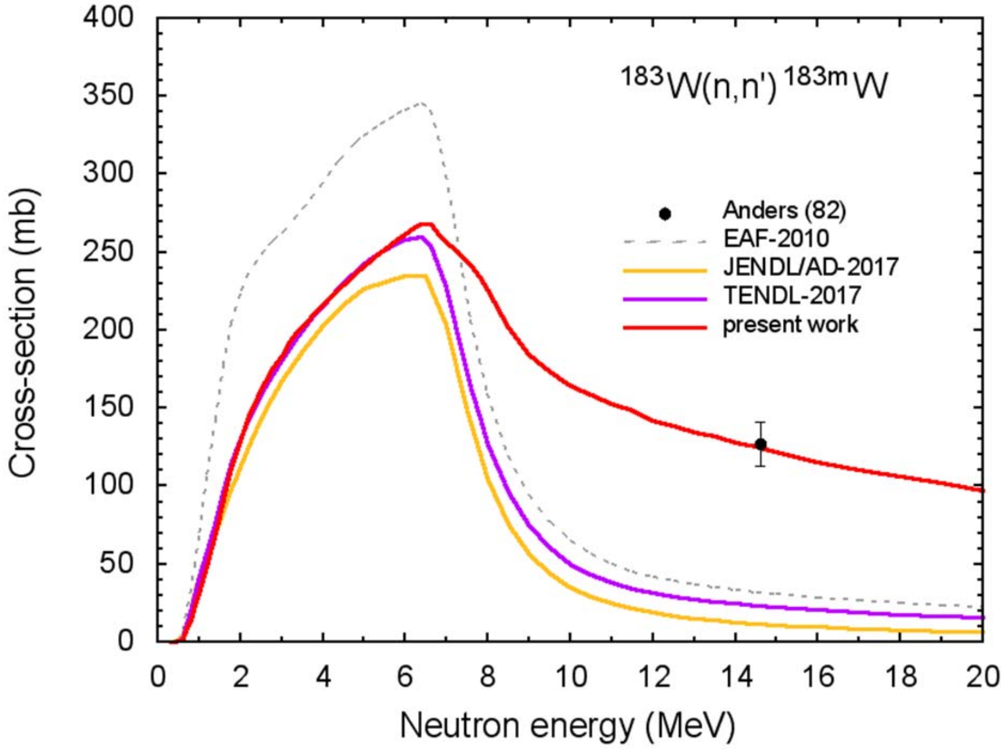

Fig.28 Inelastic scattering cross-section with production of ^{183}W isotope in the metastable state ($T_{1/2}$=5.25 s). See discussion in the text.

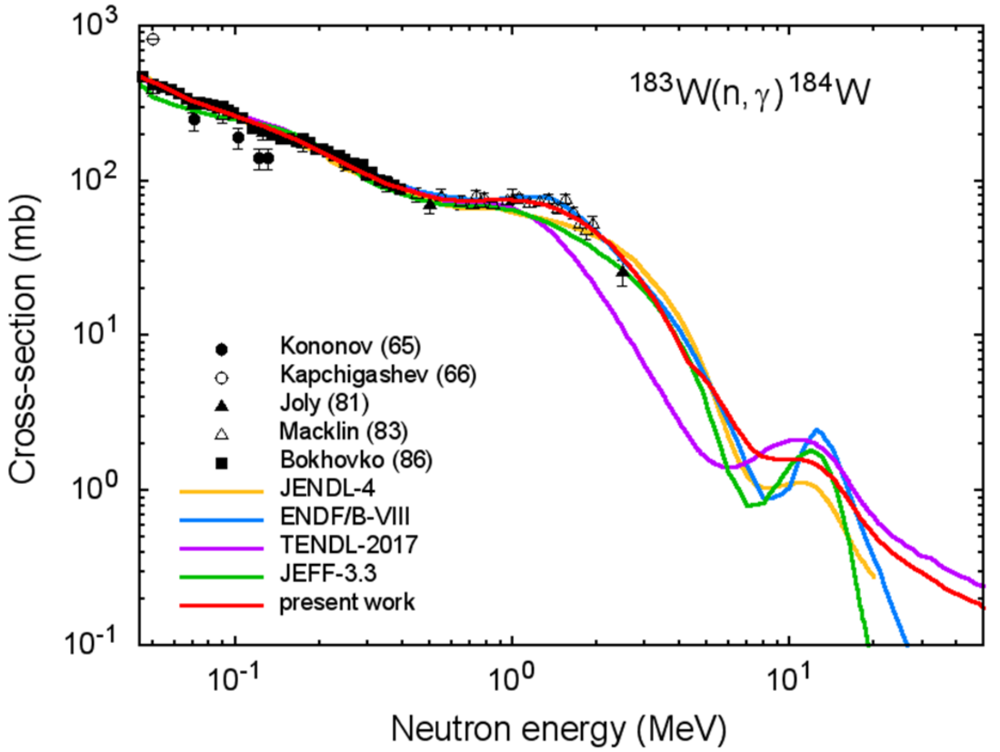

Fig.29 (n,γ) reaction cross-section for ^{183}W.

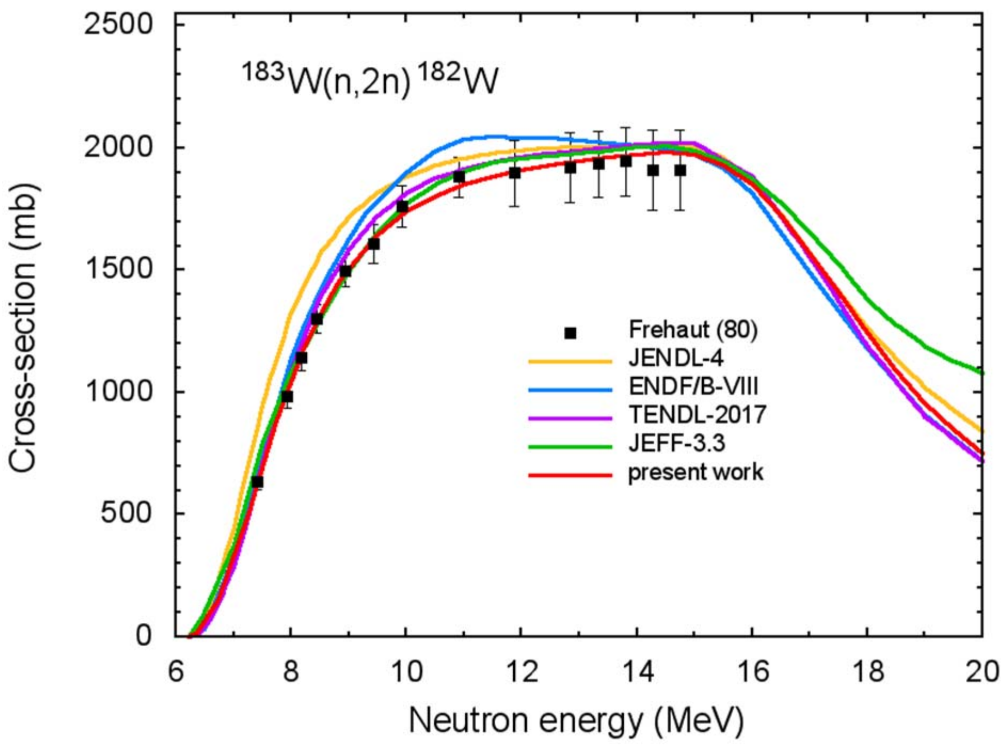

Fig.30 (n,2n) reaction cross-section for ^{183}W.

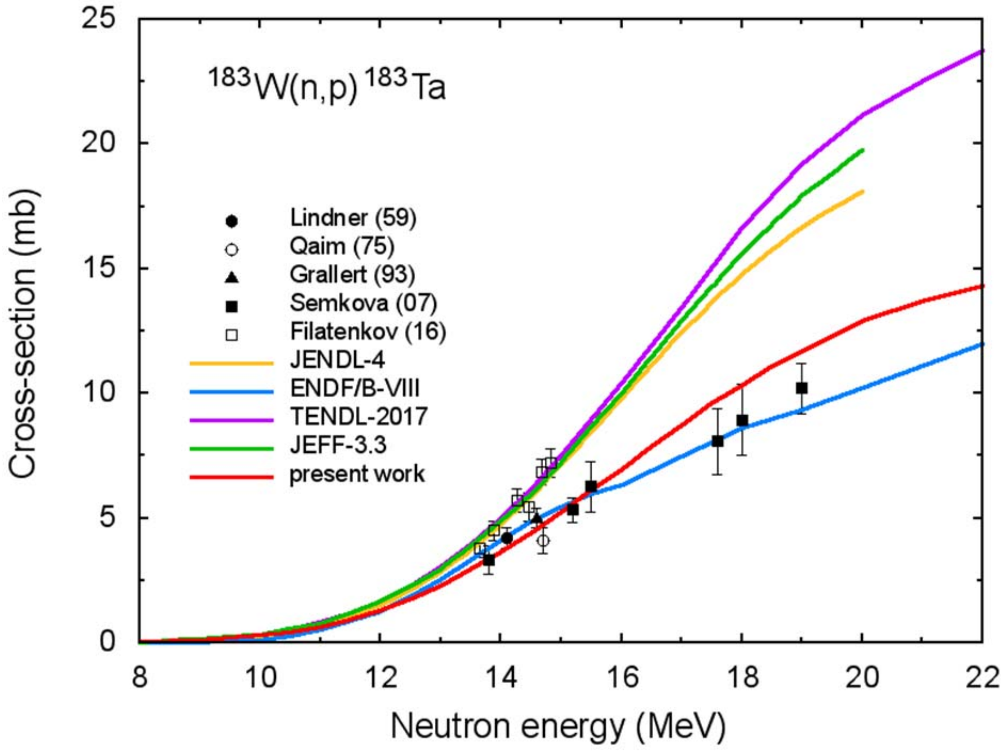

Fig.31 (n,p) reaction cross-section for ^{183}W.

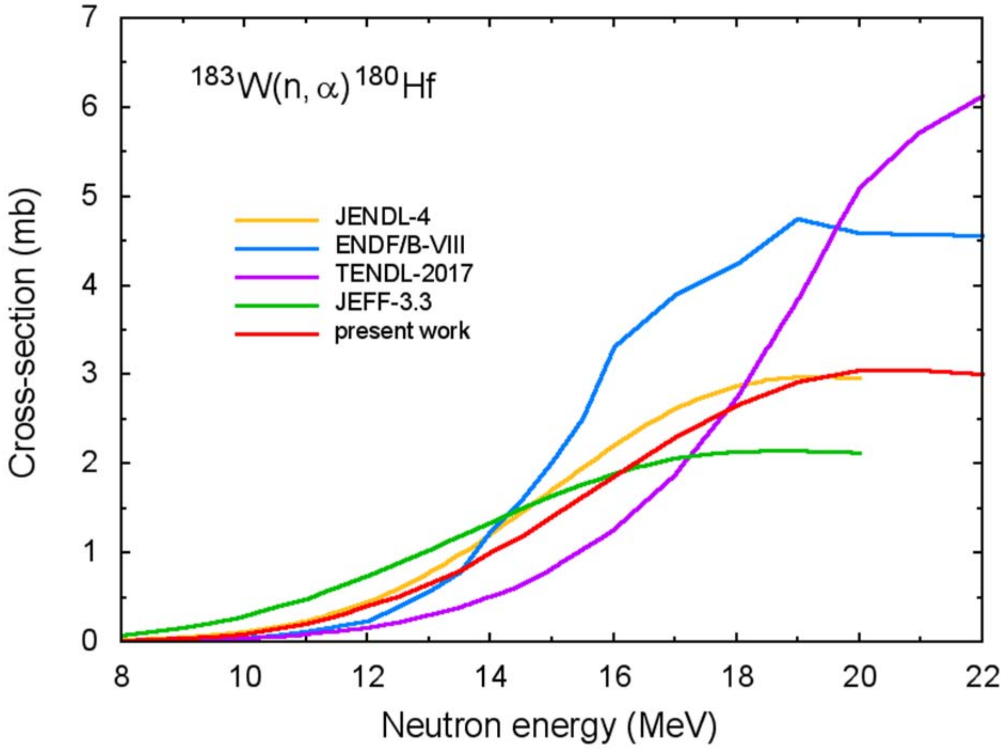

Fig.32 (n,α) reaction cross-section for ^{183}W.

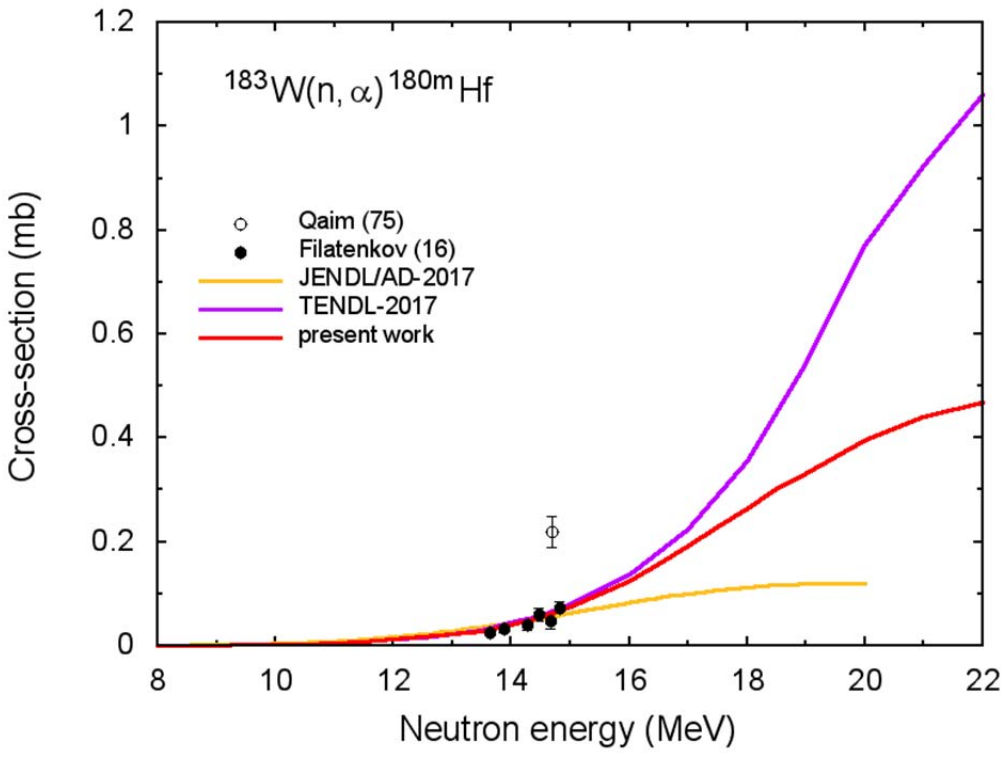

Fig.33 (n,α) reaction cross-section for ^{183}W with production of ^{180}Hf in the metastable state.

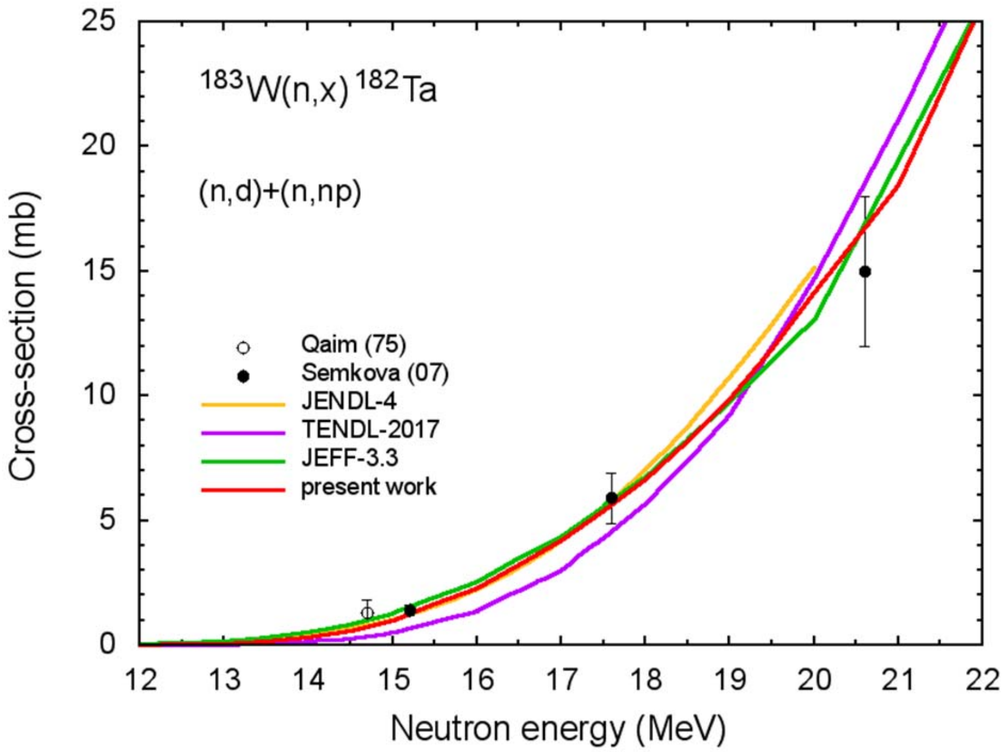

Fig.34 Sum of (n,d) and (n,np) reaction cross-section for ^{183}W.

4.5 Neutron energy distribution

Due to the lack of measurements of neutron spectra for ^{183}W, comparisons are made with experimental data for a natural mixture of tungsten isotopes, Figs.35,36. Such a comparison is, to a certain extent, conditional and, as in the case of other W-isotopes [1], can serve as a general illustration of differences, but not to check the absolute values.

The neutron energy distribution for natural tungsten calculated using data evaluated recently for tungsten isotopes [1,82] is shown in Fig.37.

4.6 Photon energy distribution

Examples of obtained photon energy distributions for neutron irradiation of ^{183}W and natural tungsten with 14 MeV neutrons are shown in Figs.38,39.

Similar to neutron spectra, Section 4.5, the Fig.38 for ^{183}W is intended for general illustrative purposes.

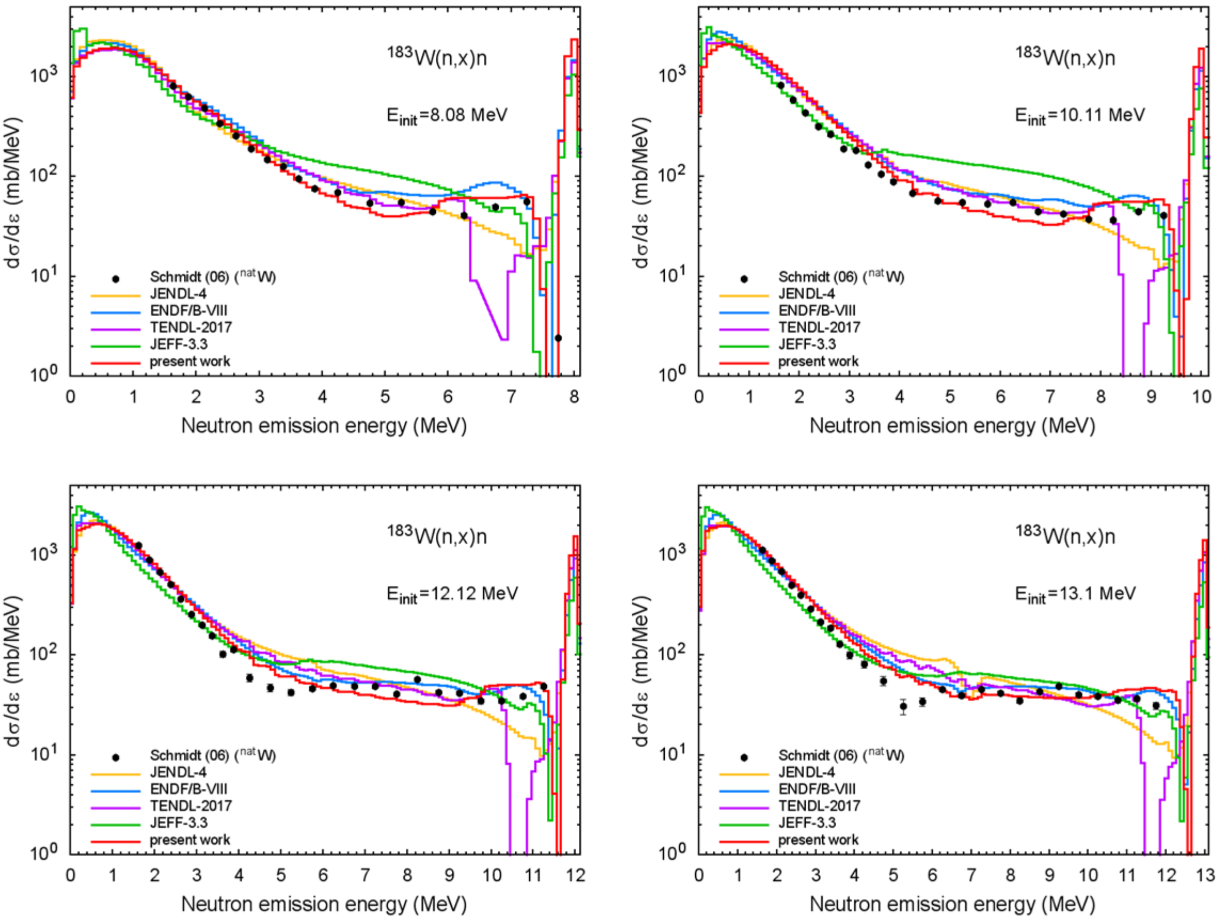

Fig.35 Neutron energy distributions for n+^{183}W reactions at different incident energies

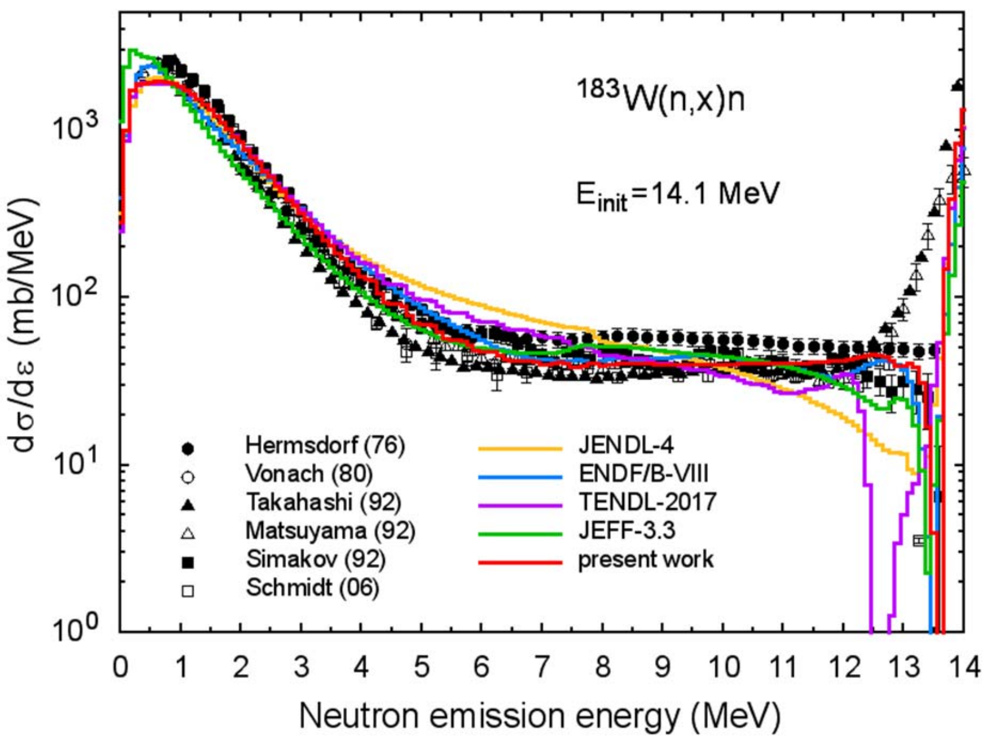

Fig.36 The same as in Fig.35 at neutron incident energy 14.1 MeV

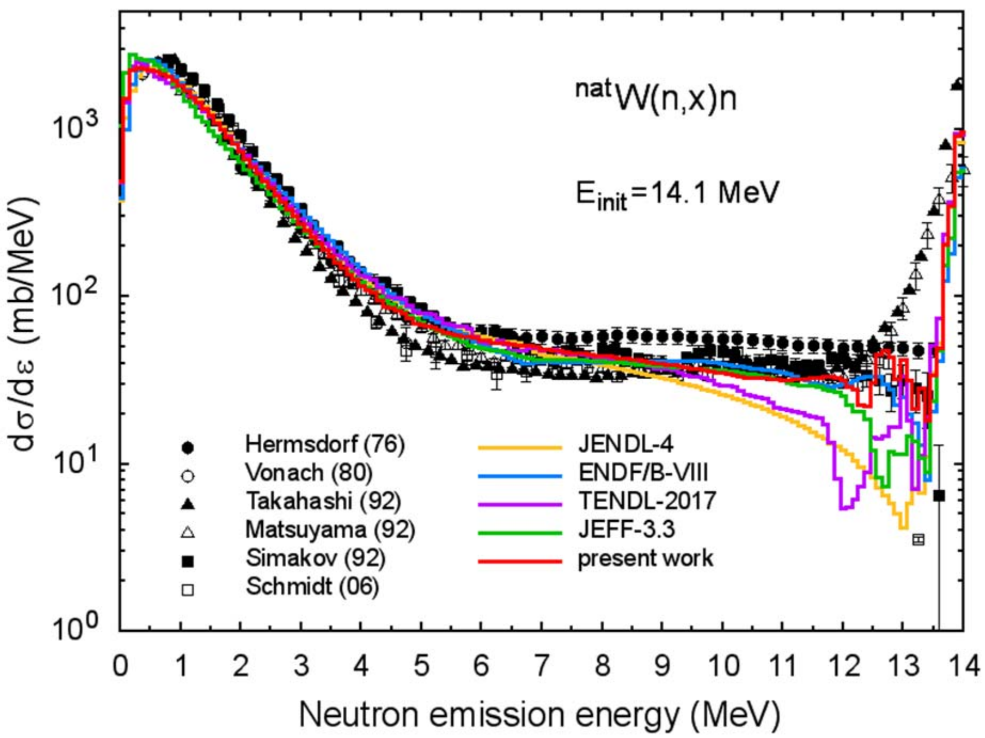

Fig.37 Neutron energy distributions for irradiation of natural tungsten with 14.1 MeV neutrons. The values marked as "present work" are obtained using data for stable tungsten isotopes: ^{180}W (this work), ^{182}W [1], ^{183}W (this work), ^{184}W [77], and ^{186}W [1].

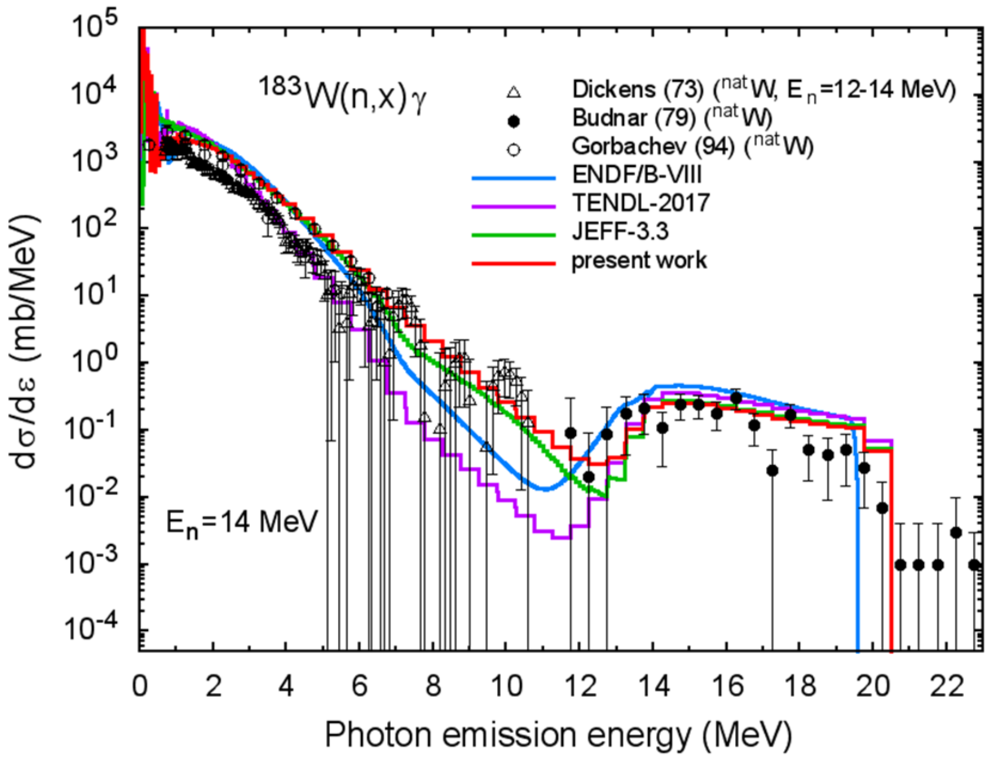

Fig.38 Photon energy distribution for n+^{183}W reactions at 14 MeV neutron energy.

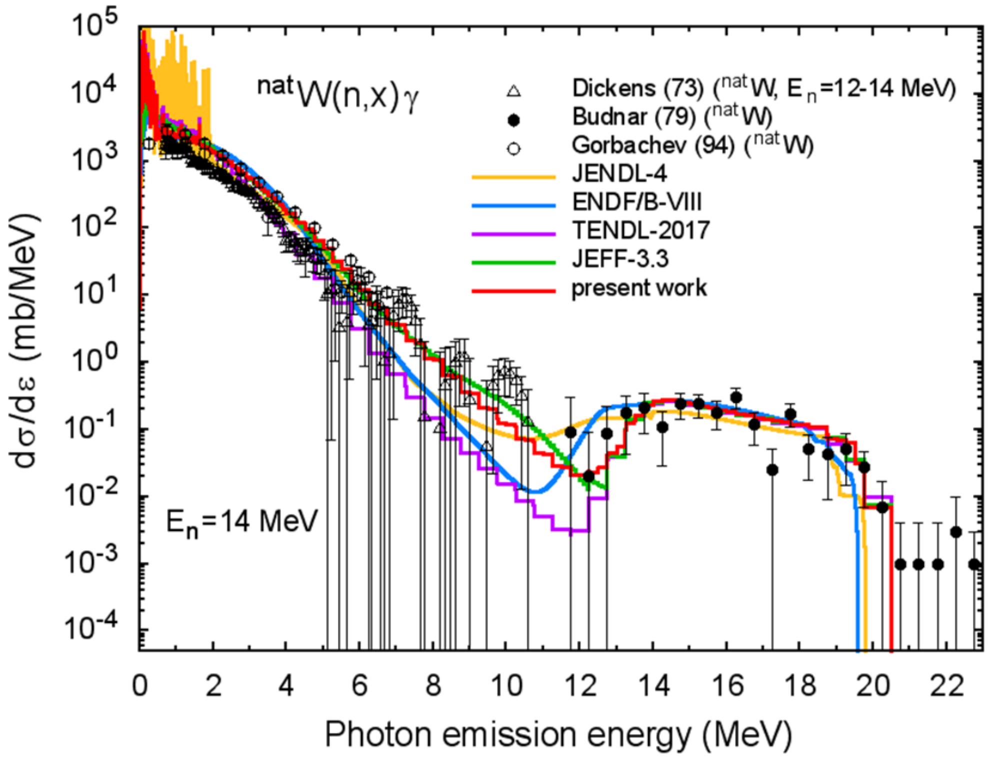

Fig.39 Photon energy distributions for irradiation of natural tungsten with 14 MeV neutrons. The values marked as "present work" are obtained using data for stable tungsten isotopes: ^{180}W (this work), ^{182}W [1], ^{183}W (this work), ^{184}W [77], and ^{186}W [1].

4.7 Light particle production cross-sections

Figures 40-45 show the neutron, proton, deuteron, triton, ^{3}He, and α-particle production cross-sections. Together with data from various libraries, Fig.40 shows results of calculations with intranuclear cascade evaporation model [72-75], and Figs.41-45 the data [57] obtained from the estimation of A-dependence of gas production cross-section components for 96 MeV neutrons, discussed in Section 2.4.

Cross-sections evaluated are in agreement with CASCADE and CEM03 calculations, Fig.40, and with the “reference” data, Figs.41-45.

4.8 Photon production cross-sections

Total photon production cross-section is plotted in Fig.46.

There is a rather large difference in the cross section values evalauated by different authors.

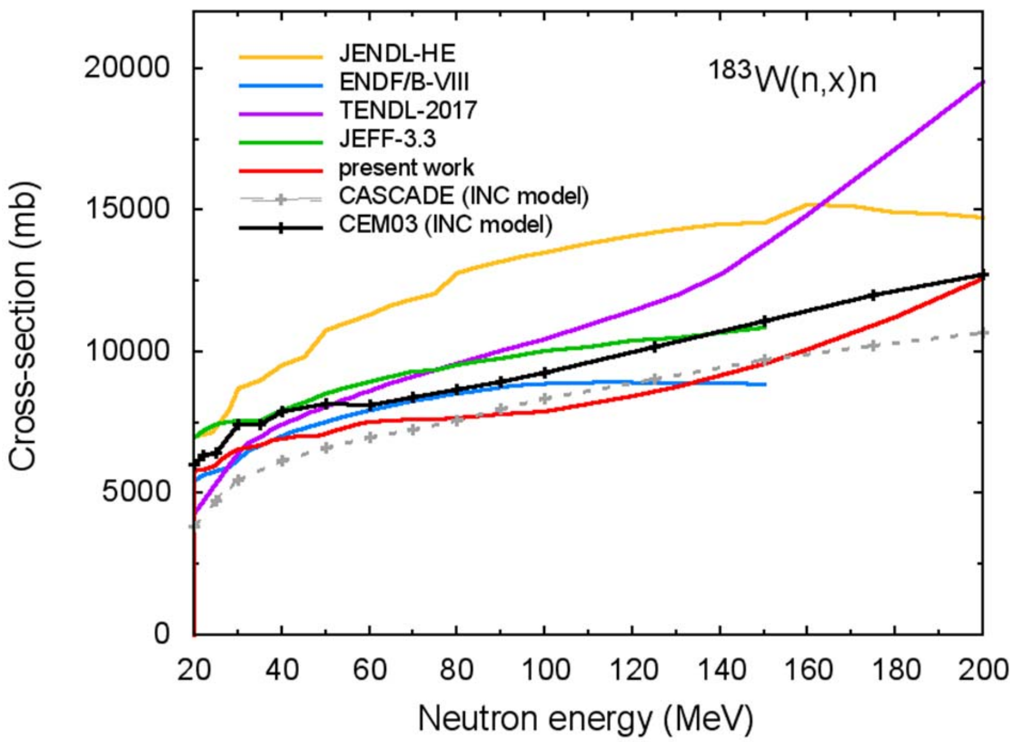

Fig.40 Neutron production cross-section for ^{183}W.

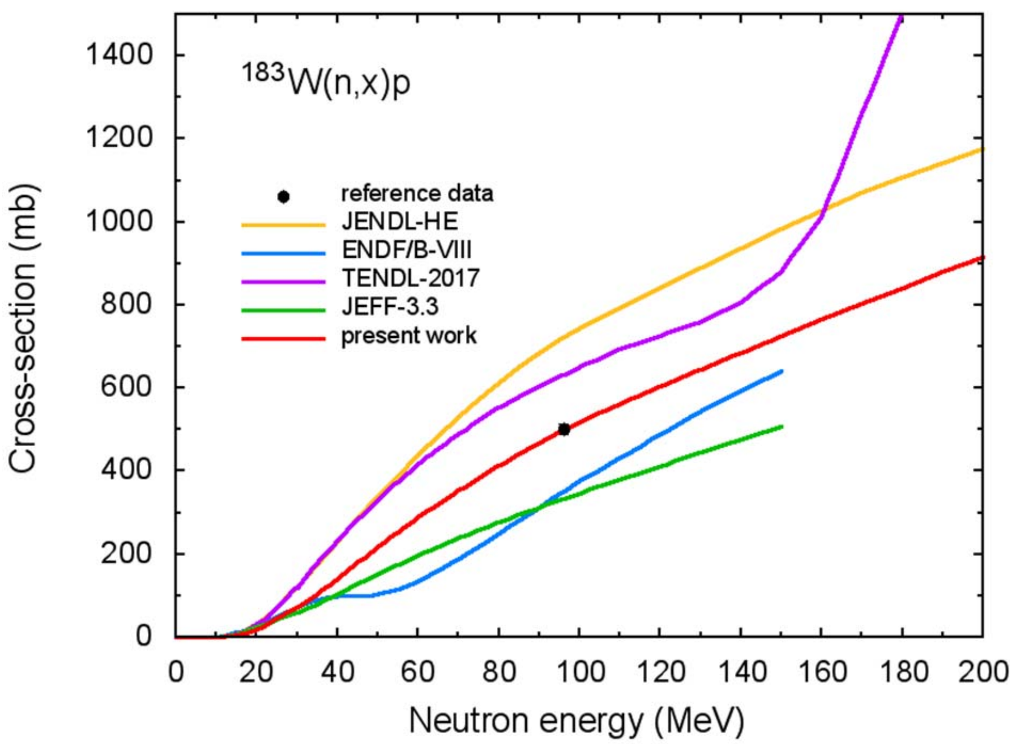

Fig.41 Proton production cross-section for ^{183}W.

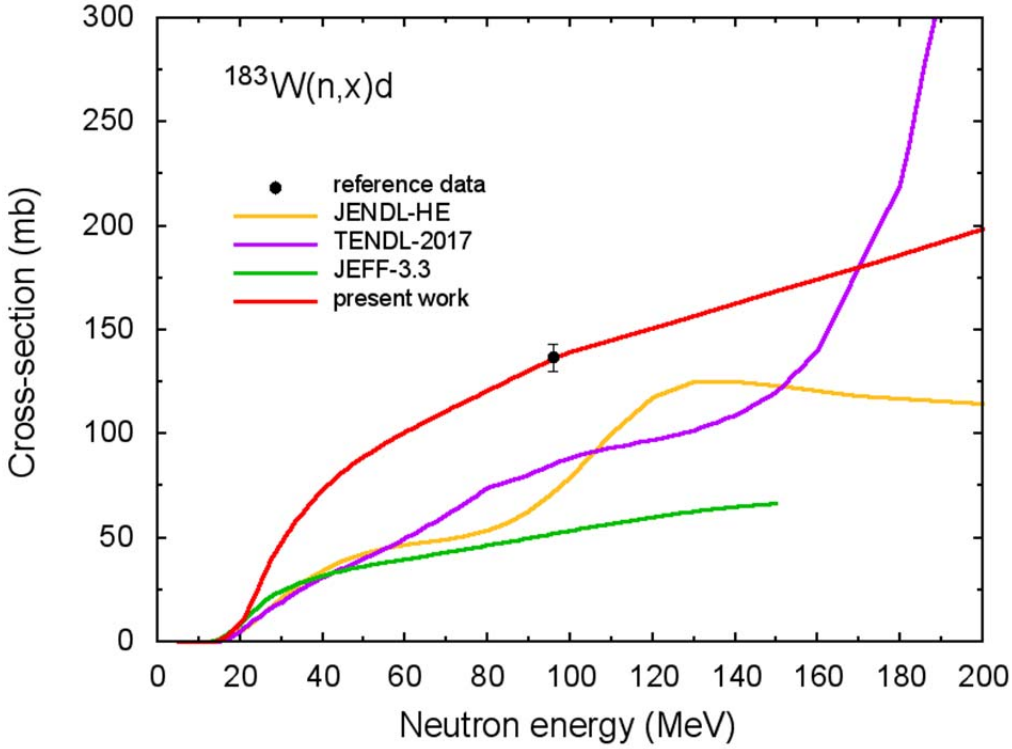

Fig.42   Deuteron production cross-section for ^{183}W.

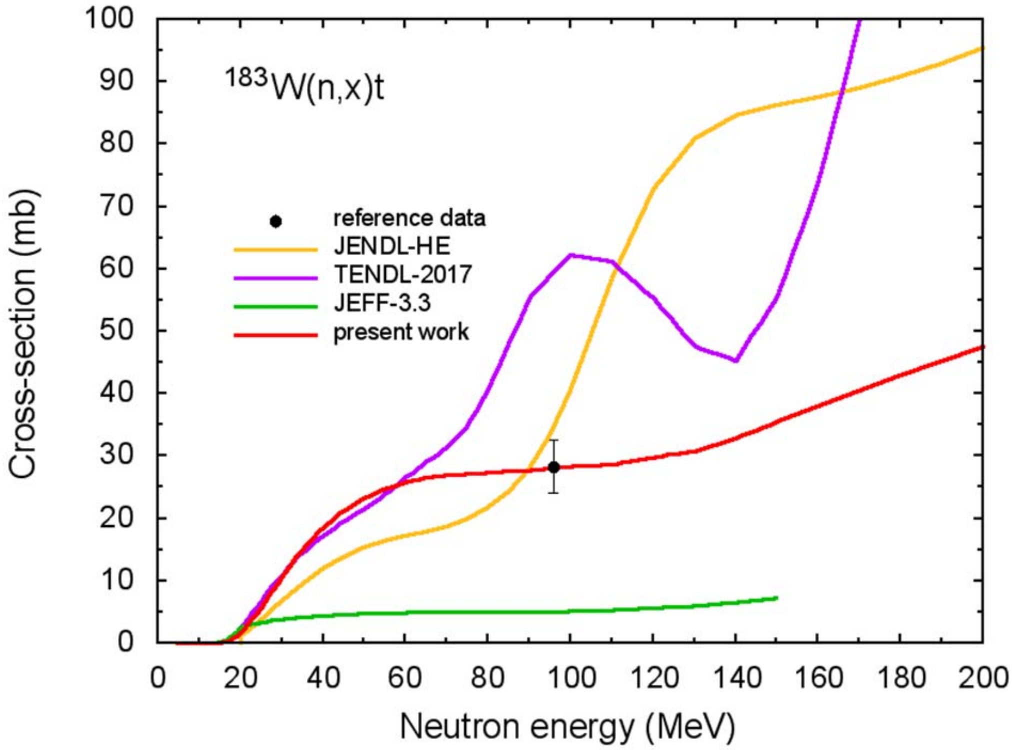

Fig.43   Triton production cross-section for ^{183}W.

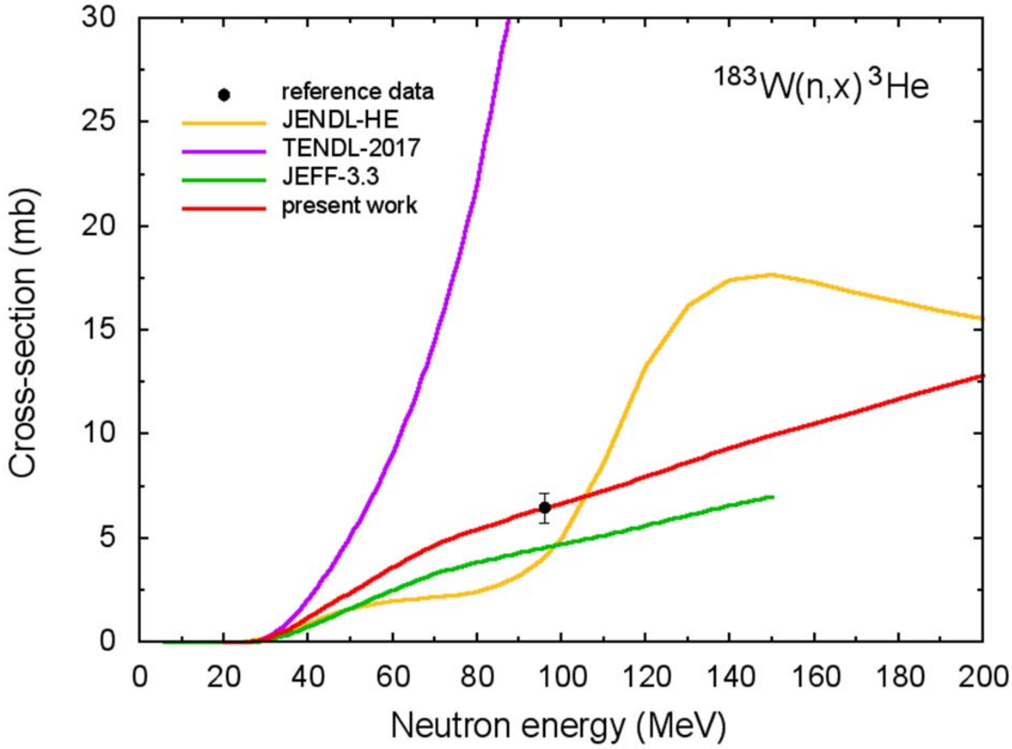

Fig.44 ^{3}He production cross-section for ^{183}W.

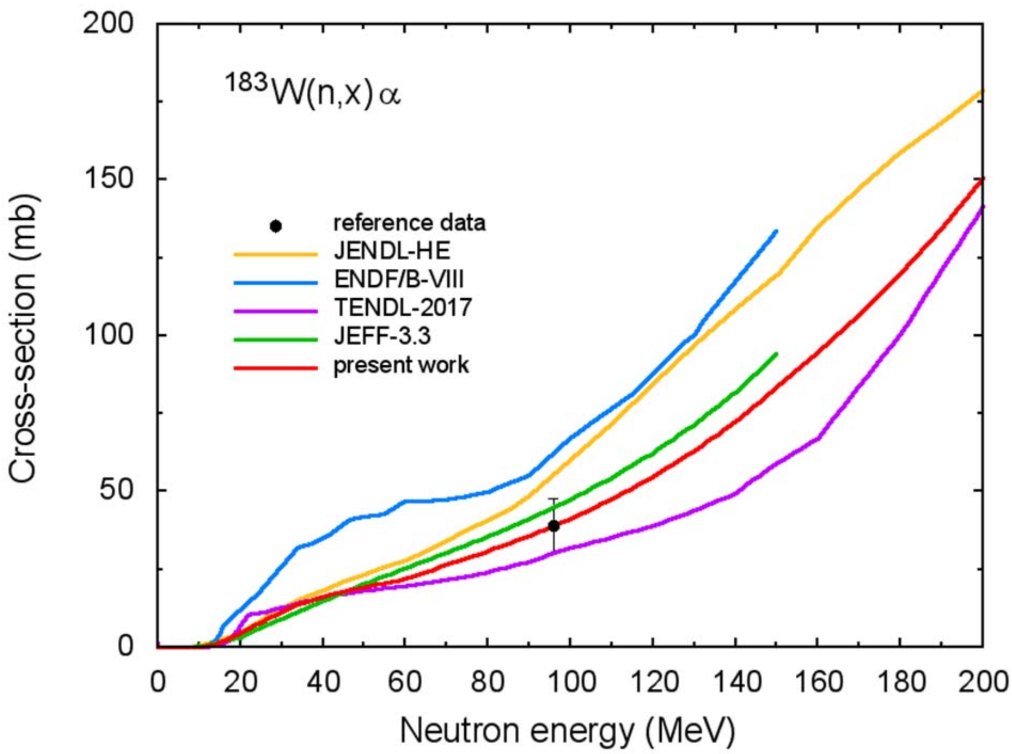

Fig.45 α-particle production cross-section for ^{183}W.

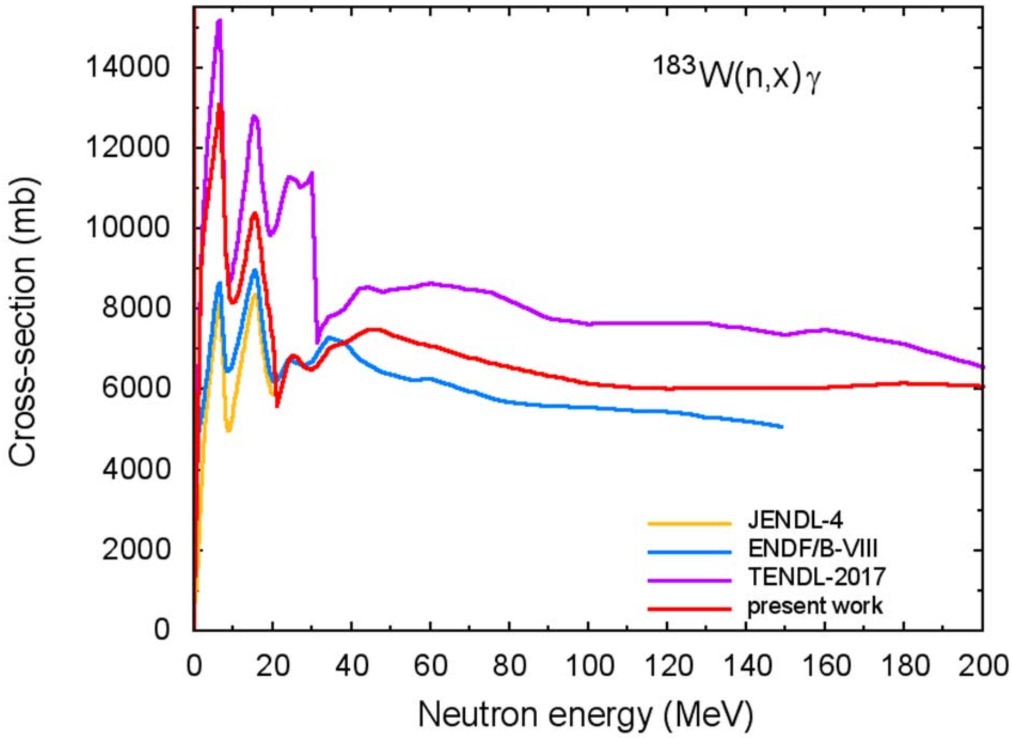

Fig.46 Photon production cross-section for ^{183}W.

4.9 Atomic displacement cross-section

Figure 47 shows the displacement cross-section for ^{183}W obtained using evaluated data processed with NJOY. For comparison cross-sections from various libraries and σ_d values calculated using the CEM03 code with the added elastic component of the cross-section are also shown.

Obtained cross-sections agree with TENDL-2017 data at energies up to 100 MeV and with cross-sections calculated using the CEM03 code at different energies.

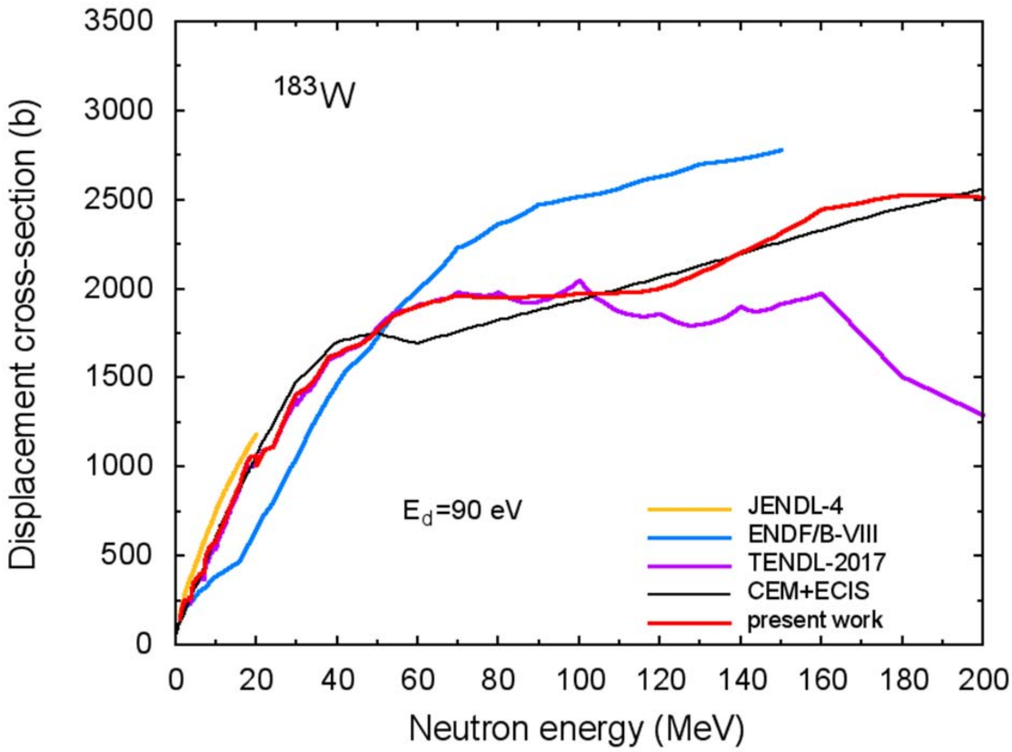

Fig.47 Atomic displacement cross-section for ^{183}W.

5.0 Covariance matrices

Figure 48 shows examples of covariance matrices for the inelastic scattering cross-section (n,n)' and (n,2n) reaction cross-section obtained using results of model calculations and experimental data. Calculations were performed using BEKED.

5. CONCLUSION

New general purpose data files were prepared for ^{180}W and ^{183}W at incident neutron energies up to 200 MeV. A special version of the TALYS code implementing the geometry dependent hybrid model and models for non-equilibrium cluster emission was applied for calculations of reaction cross-sections and particle energy distributions.

The evaluation of cross-sections was performed using available measured data, data of systematics, and obtained covariance information.

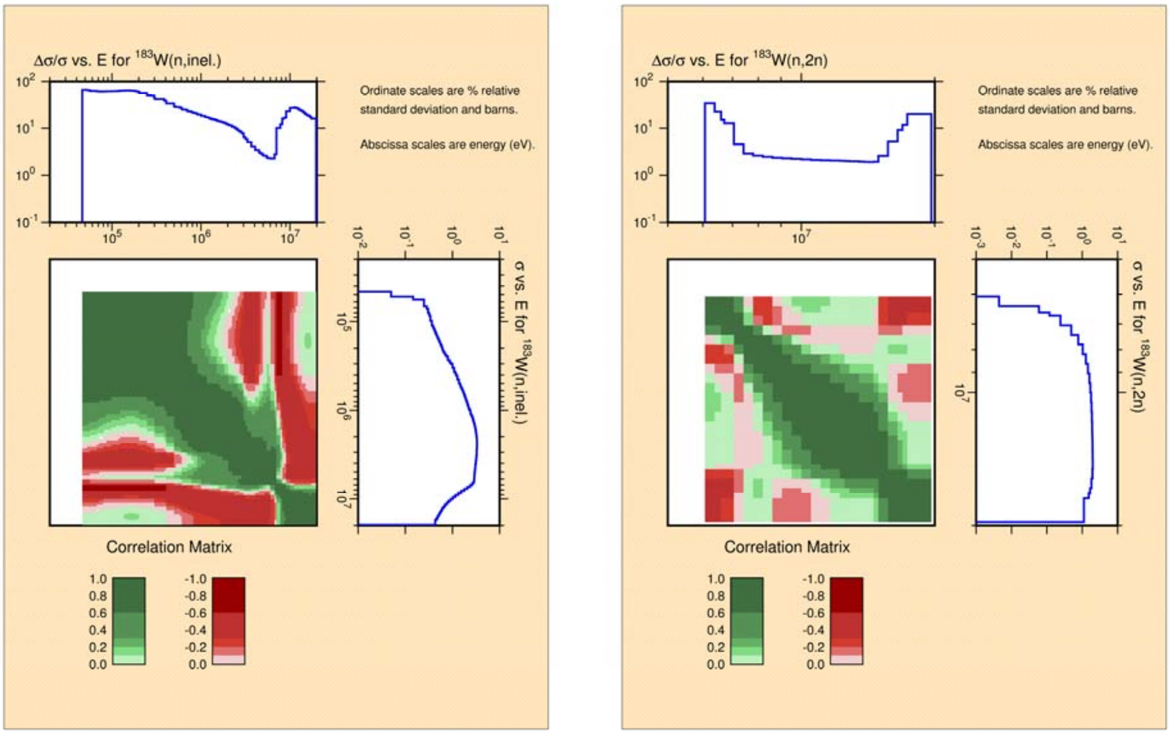

Fig.48 Example of covariance matrices calculated for neutron inelastic scattering cross-section (n,n)’ and (n,2n) reaction cross-section for ^{183}W. Plots were prepared using the NJOY code.

Acknowledgement

This work has been carried out within the framework of the EUROfusion Consortium and has received funding from the Euratom research and training programme 2014-2018 and 2019-2020 under grant agreement No 633053. The views and opinions expressed herein do not necessarily reflect those of the European Commission.

References

[1] A.Yu. Konobeyev, U. Fischer, P.E. Pereslavtsev, S.P. Simakov, Evaluated data files for neutron irradiation of ^{182}W and ^{186}W at energies up to 200 MeV, Report KIT SWP 108 (2019); https://publikationen.bibliothek.kit.edu/1000090132

[2] A.J. Koning, S. Hilaire, M. Duijvestijn, TALYS-1.7, A nuclear reaction program, Nuclear Research and Consultancy Group (NRG), May 7, 2015

[3] A.Yu. Konobeyev, U. Fischer, P.E. Pereslavtsev, A. Koning, M. Blann, Implementation of GDH model in TALYS-1.7 code, Report KIT SWP 45 (2016); https://publikationen.bibliothek.kit.edu/1000052543

[4] M. Blann, H.K. Vonach, Global test of modified precompound decay models, *Phys. Rev. C* 28 (1983) 1475

[5] A.Yu. Konobeyev, U. Fischer, A.J. Koning, P.E. Pereslavtsev, M. Blann, Implementation of the geometry dependent hybrid model in TALYS, *J. Korean Physical Society* 59 (2011) 935

[6] C.H.M. Broeders, A.Yu. Konobeyev, A.Yu. Korovin, V.P. Lunev, M. Blann, ALICE/ASH - Pre-compound and evaporation model code system for calculation of excitation functions, energy and angular distributions of emitted particles in nuclear reactions at intermediate energies, Report FZKA 7183, May (2006), http://bibliothek.fzk.de/zb/berichte/FZKA7183.pdf

[7] A.J. Koning, J.P. Delaroche, Local and global nucleon optical models from 1 keV to 200 MeV, *Nucl. Phys.* A713 (2003) 231.

[8] D.A. Brown, M.B. Chadwick, R. Capote, A.C. Kahler, A. Trkov, M.W. Herman, A.A. Sonzogni, Y. Danon, A.D. Carlson, M. Dunn, D.L. Smith, G.M. Hale, G. Arbanas, R. Arcilla, C.R. Bates, B. Beck, B. Becker, F. Brown, R.J. Casperson, J. Conlin, D.E. Cullen, M.-A. Descalle, R. Firestone, T. Gaines, K.H. Guber, A.I. Hawari, J. Holmes, T.D. Johnson, T. Kawano, B.C. Kiedrowski, A.J. Koning, S. Kopecky, L. Leal, J.P. Lestone, C. Lubitz, J.I. Márquez Damián, C.M. Mattoon, E.A. McCutchan, S. Mughabghab, P. Navratil, D. Neudecker, G.P.A. Nobre, G. Noguere, M. Paris, M.T. Pigni, A.J. Plompen, B. Pritychenko, V.G. Pronyaev, D. Roubtsov, D. Rochman, P. Romano, P. Schillebeeckx, S. Simakov, M. Sin, I. Sirakov, B. Sleaford, V. Sobes, E.S. Soukhovitskii, I. Stetcu, P. Talou, I. Thompson, S. van der Marck, L. Welser-Sherrill, D. Wiarda, M. White, J.L. Wormald, R.Q. Wright, M. Zerkle, G. Žerovnik, Y. Zhu, ENDF/B-VIII.0: The 8^{th} major release of the nuclear reaction data library with CIELO-project cross sections, new standards and thermal scattering data, *Nuclear Data Sheets,* 148 (2018) 1.

[9] D.L. Smith, Covariance matrices for nuclear cross sections derived from nuclear model calculations, Report ANL/NDM-159 (2004).

[10] A.Yu. Konobeyev, U. Fischer, P.E. Pereslavtsev, Computational approach for evaluation of nuclear data including covariance information, Proc. Int. Conf. Nucl. Data for Sci. and Technology, Jeju Island, Korea (2010).

[11] A.J. Koning, D. Rochman, Modern nuclear data evaluation with the TALYS code system, *Nucl. Data Sheets,* 113 (2012) 2841.

[12] A.J. Koning, TEFAL-1.9: Making nuclear data libraries using TALYS, Nuclear Research and Consultancy Group (NRG) (2017)

[13] B. Anders[1], R. Pepelnik, H.-U. Fanger, Application of a novel 14 MeV neutron activation analysis system for cross section measurements with short-lived nuclides, Proc. Conf. on Nucl. Data for Sci. and Technol., Antwerp 1982, p.859 (1982).

[14] J.R.M. Annand, R.B. Galloway, Neutron analysing powers and a low-energy optical model analysis, *J. Phys.*, G11 (1985) 1341.

[15] M. Baba, H. Wakabayashi, N. Ito, K. Maeda, N. Hirakawa, Measurement of double-differential neutron emission spectra from uranium-238, J. Nucl. Sci. Technol., 31 (1994) 757, see “status” of the data for EXFOR “subnet” 22352007.

[16] R.L. Becker, W.G. Guindon, G.J. Smith, Elastic scattering of 3.2 MeV neutrons from many elements, *Nucl. Phys.*, 89 (1966) 154.

[17] F. Becvar, R.E. Chrien, O.A. Wasson, The study of neutron resonance capture in ^{149}Sm, *Bulletin of the American Physical Society,* 15 (1970) 1667.

[18] R.C. Block, R.W. Hockenbury, J.E. Russell, The parameters of the neutron resonances in ^{182}W, ^{183}W, ^{184}W, and ^{186}W, Rensselaer Polytechnic Inst. Reports, No.328-56, p.14 (1966); Report ORNL-3778, p.53 (1965).

[19] M.V. Bokhovko, L.E. Kazakov, V.N. Kononov, E.D. Poletaev, V.M. Timokhov, A.A. Voevodskiy, The measurement of the neutron capture cross-section for tungsten isotopes in the energy range from 5 to 400 keV, Report INDC(CCP)-259, p.39 (1986); *Vopr. At. Nauki i Tekhn., Ser. Yadernye Konstanty*, Issue.1, (1986) p.39; *Yadernaya Fizika* 46 (1987) 51, Engl. translation: *Soviet Journal of Nuclear Physics* 46 (1987) 33.

[20] M. Budnar, F. Cvelbar, E. Hodgson, A. Hudoklin, V. Ivkovic, A. Likar, M.V. Mihailovic, R. Martincic, M. Najzer, A. Perdan, M. Potokar, V. Ramsak, Prompt γ-ray spectra and integrated cross sections for the radiative capture of 14 MeV neutrons for 28 natural targets in the mass region from 12 to 208, Report INDC(YUG)-6/L (1979).

[21] Cao Jianhua, Dai Yunsheng, Wan Dairong, Liang Xuecai,Wang Shiming, Differential elastic scattering cross sections of the fast neutrons from Mo, Nb and W, Report INDC(CPR)-011, p.125 (1988).

[22] S.A. Cox, E.E. Dowling Cox, Polarization in the elastic scattering of neutrons from medium- and heavy-weight elements, Report ANL-7935 (1972).

[23] J.P. Delaroche, G. Haouat, J. Lachkar, Y. Patin, J. Sigaud, J. Chardine, Deformations, moments, and radii of ^{182,183,184,186}W from fast neutron scattering, *Phys. Rev.*, C23 (1981) 136.

[1] The experimental works from Ref.[13] to Ref.[58] are listed in alphabetical order

[24] J.K. Dickens, G.L. Morgan, G.T. Chapman, T.A. Love, E. Newman, F.G. Perey, Cross sections for gamma-ray production by fast neutrons for 22 elements between Z = 3 and Z = 82, Oak Ridge National Lab. Reports, No.4847 (1973); *Nucl. Sci. Eng.,* 62 (1977) 515.

[25] F.S. Dietrich, J.D. Anderson, R.W. Bauer, S.M. Grimes, R.W. Finlay, W.P. Abfalterer, F.B. Bateman, R.C. Haight, G.L. Morgan, E. Bauge, J.P. Delaroche, P. Romain, Importance of isovector effects in reproducing neutron total cross section differences in the W isotopes, *Phys. Rev.,* C67 (2003) 044606

[26] D.M. Drake, J.C. Hopkins, C.S. Young, Gamma-ray-production cross sections for fast neutron interactions with several elements, *Nucl. Sci. Eng.*, 40 (1970) 294.

[27] A.A. Filatenkov, Neutron activation cross sections measured at KRI in neutron energy region 13.4 - 14.9 MeV, Report INDC(CCP)-0460 (2016).

[28] J. Frehaut, A. Bertin, R. Bois, J.Jary, G. Mosinski, Status of (n,2n) cross section measurements at Bruyeres-le-Chatel, INDC(USA)-84,(1), p.399 (1980), Revised data: Report CEA-R-6447 (2016).

[29] S.J. Friesenhahn, E. Haddad, F.H. Froehner, W.M. Lopez, The neutron capture cross section of the tungsten isotopes from 0.01 to 10 electron Volts, *Nucl. Sci. Eng.* 26, (1966) 487.

[30] V.M. Gorbachev, V.I. Nagorny, Yu.Ya. Nefedov, M.S. Shvetsov, E.F. Fomushkin, A.M. Shvetsov, Gamma-ray production cross-section for interactions of 13.8 MeV neutrons with Cu, W and ^{235}U nuclei, Proc. Intern. Conf. Nuclear Data for Science and Technology, Gatlinburg, Tennesse, 9-13 May, 1994, J.K.Dickens, Ed.; American Nuclear Society, Vol.2, (1994) p.950; *Vopr. At.Nauki i Tekhn., Ser.Yadernye Konstanty*, Issue.2 (1996) p.47.

[31] A. Grallert, J. Csikai, Cs.M. Buczko, I. Shaddad, Investigations on the systematics in (n,α) cross sections at 14.6 MeV, Report INDC(NDS)-286, p.131 (1993).

[32] D. Hermsdorf, A. Meister, S. Sassonoff, D. Seeliger, K. Seidel, Absolute differentielle Neutronenemissionsquerschnitte für Ga, Se, Br,Zr, Nb, Cd, In, Sn, Sh, J, Ta, W, Au, Hg, Pb und Bi bei 14 MeV Einschussenergie, Kernenergie, 19 (1976) 241.

[33] C.E. Hollandsworth, W.P. Bucher, J. Youngblood, A. Niiler, Cross sections for forward-angle elastic scattering of 7.55 mev neutrons- a survey, Ballistic Research Labs Reports, No.1764 (1975).

[34] S. Joly, J. Voignier, G. Grenier, D.M. Drake, L. Nilsson, Measurement of fast neutron capture cross sections using a Na-I spectrometer, Report CEA-R-5089 (1981).

[35] Kaihong Fang, Yang Xiang, Yuncheng Han, Xiangzhong Kong, Tieshan Wang, Rong Liu, Li Jiang, Measurements of activation cross-sections for $^{165}Ho(n,2n)^{164g}Ho$ and $^{180}W(n,2n)^{179g}W$ reactions induced by neutrons around 14 MeV, *Radiation Measurements*, 44 (2009) 68.

[36] Kaihong Fang, Shiwei Xu, Changlin Lan, Xiaosan Xu,Xiangzhong Konga, Rong Liu, Li Jiang, Cross-section measurement for the reactions producing short-lived nuclei induced by neutrons around 14 MeV, *Appl. Rad. Isot.*, 66 (2008) 1104.

[37] W.G. Kang, Y.D. Kim, J.I. Lee, I.S. Hahn, A.R. Kim,H.J. Kim, Measurement on the thermal neutron capture cross section of ^{180}W, *Phys. Rev.*, C76 (2007) 067602.

[38] S.V. Kapchigashev, Yu.P. Popov, F.L. Shapiro, Radiative capture cross-sections measurements for neutrons in the energy range up to 50 keV for elements with even proton number, Priv. Comm: Kapchigashev (1966), *Atomnaya Energiya*, 15 (1963) 120, Engl. transl.: *Soviet Atomic Energy*, 15, (1964) 808.

[39] K. Knopf, W. Waschkowski, Interaction of neutrons with tungsten and its isotopes, *Zeitschrift für Naturforschung*, A42 (1987) 909.

[40] V.N. Kononov, Yu.Ya. Stavissky, V.E. Kolesov, A.G. Dovbenko, V.S. Nesterenko, V.I. Moroka, Radiative capture cross sections of 30-170 keV neutrons, Report FEI-29 (1965); *Yadernaya Fizika* 4 (1966) 282, English. transl. *Soviet Journal of Nuclear Physics*, 4 (1967) 204; *Atomnaya Energiya,* 19 (1965) 457, Engl. transl.: *Soviet Atomic Energy*, *19* (1965) 1428.

[41] A.I. Lashuk, I.P. Sadokhin, Gamma-quanta production cross sections at neutron inelastic scattering at the energy 3 MeV, *Vopr. At. Nauki i Tekhn., Ser. Yadernye Konstanty*, Issue.2 (1996) p.59; *Vopr. At. Nauki i Tekhn., Ser. Yadernye Konstanty*, Issue.1 (1994), p.26.

[42] M. Lindner, J. Miskel, Miscellaneous Neutron Reaction Cross Sections, Washington AEC Office Reports, No.1018, p.63 (1959).

[43] Ma Gonggui, Zou Yiming, Xie Daquan, Wang Shiming, Li Jingde, Chen Shuying, Fast neutron small angle elastic scattering researches, Report INDC(CPR)-11, p.135 (1988); *Chinese J. of Nuclear Physics*, 9 (1987) 97.

[44] R.L. Macklin, D.M. Drake, E.D. Arthur, Neutron Capture Cross Sections of ^{182}W, ^{183}W, ^{184}W, and ^{186}W from 2.6 to 2000 keV, *Nucl. Sci. Eng.* 84 (1983) 98.

[45] S. Matsuyama, T. Okubo, M. Baba, T. Ito, T. Akiyama, N. Ito, N. Hirakawa, Measurement of double-differential neutron emission cross sections of Mo, Ta and W, Report JAERI-M-93-046, p.345 (1992), Report INDC(JPN)-163/L, p.345 (1992), J. Nucl. Sci. Technol., 27 (1990) 601.

[46] M. Ohkubo, Y. Kawarasaki, Total cross sections of tungsten, sodium and bromine, Priv. Comm: Ohkubo (1978).

[47] S. Pearlstein, E.J. Winhold, Inelastic scattering of 14 MeV neutrons to low-lying states of Ta, W, Tl, and Pb, *J. Nuclear Energy A&B (Reactor Sci. and Technol.)*, 19 (1965) 497.

[48] S.M. Qaim, C. Graca, Neutron activation cross sections at 14.7 MeV for isotopes of tungsten, *Nucl. Phys.*, A242 (1975) 317.

[49] M.V. Savin, Ju.A. Khokhlov, I.N. Paramonova, V.A. Chirkin, V.N. Ludin, N.N. Zaljalov, Total gamma-production cross-section in the (n,x-gamma) reaction on the tungsten in the neutron energy range 1 - 10 MeV, Yaderno-Fizicheskie Issledovaniya Reports, Moscow, No.27, (1979), p.5.

[50] D. Schmidt, W. Mannhart, S. Khurana, Determination of differential elastic and double-differential neutron scattering cross sections of elemental tungsten at energies between 7.19 MeV and 14.10 MeV, Phys. Techn. Bundesanst., Neutronenphysik Reports, No.51 (2006).

[51] W. Selove, Resonance-region neutron spectrometer measurements on silver and tungsten, *Phys. Rev.*, 84 (1951) 869.

[52] V. Semkova, R. Capote, R.J. Tornin, A.J. Koning, A. Moens, A.J.M. Plompen, New cross section measurements for neutron-induced reactions on Cr, Ni, Cu, Ta and W isotopes obtained with the activation technique, Proc. Conf. on Nucl. Data for Sci. and Technology, Nice 2007, Vol.1, p.559 (2007); *Nucl. Phys.*, A730 (2004) 255.

[53] S.P. Simakov, B.V. Devkin, M.G. Kobosev, A.A. Lychagin, V.A. Talalaev, C. Sandin, Differential neutron emission cross-sections for beryllium and tangsten at 14 MeV incident neutron energy, Report INDC(NDS)-272, p.131 (1992).

[54] A. Takahashi, Y. Sasaki, F. Maekawa, H. Sugimoto, Measurement of double, single differential and integral neutron emission cross sections at 14.1 MeV for Ca-nat, Mn-55, Co-59, and W-nat, Osaka Univ., OKTAVIAN Reports, No.92-01 (1992).

[55] K. Tsukada, S. Tanaka, Y. Tomita, M. Maruyama, Elastic and inelastic scattering of fast neutrons from iron, nickel and tungsten, *Nucl. Phys.*, A125 (1969) 641.

[56] W.E. Tucker, P.S. Buchanan, T.C. Martin, D.O. Nellis, G.H. Williams, Neutron induced gamma-ray production cross sections for silicon and tungsten, Defense Atomic Support Agency Reports, No.2333 (1969).

[57] H. Vonach, A. Chalupka, F. Wenninger, G. Staffel, Measurement of the angle-integrated secondary neutron spectra from interaction of 14 MeV neutrons with medium and heavy nuclei, Report INDC(USA)-84,(1), p. 343 (1980); Conf. Brookhaven National Laboratory Reports, No.51245, Vol.(1), p.343 (1980); Conf. Zentralinst. für Kernforschung Rossendorf Reports, No.382, p.159 (1979).

[58] P.N. Vorona, O.I. Kalchenko, V.G. Krivenko, Experimental investigations of neutron cross-sections of tungsten isotope atomic nuclei: radioactive W-181 ($T_{1/2}$ =121.2 days) and stable W-180, Proc. 2 Int. Conf. Cur. Prob. in Nucl. Phys. Atom. Ene., Kyiv, 2008, p.528 (2008).

[59] Experimental Nuclear Reaction Data (EXFOR) (2019), https://www-nds.iaea.org/exfor/exfor.htm

[60] V.S. Barashenkov, A. Polanski, Electronic Guide for Nuclear Cross-Sections, Joint Institute for Nuclear Research Communication E2-94-417, JINR, Dubna, Russia, 1994.

[61] L.M. Kerby, S.G. Mashnik, Total reaction cross sections in CEM and MCNP6 at intermediate energies, Nuclear Instruments and Methods in Physics Research B 356–357 (2015) 135–145

[62] A.Yu. Konobeyev, U. Fischer, Complete gas production data library for nuclides from Mg to Bi at neutron incident energies up to 200 MeV, Report KIT SWP 36 (2015), http://digbib.ubka.uni-karlsruhe.de/volltexte/1000049466; http://goo.gl/F8hKLN

[63] A.Yu. Konobeyev, U. Fischer, Reference data for evaluation of gas production cross-sections in proton induced reactions at intermediate energies, KIT SR 7660 (2014), www.ksp.kit.edu/download/1000038463; http://goo.gl/26Vjzl

[64] D.L. Smith, A Least-squares computational tool kit, Report ANL/NDM-128, Argonne National Laboratory (1993)

[65] ENDF-6 Checking & Utility Codes, https://www-nds.iaea.org/public/endf/utility/

[66] A. Trkov, Program COVEIG, https://www-nds.iaea.org/IRDFF/coveig.for

[67] The NJOY Nuclear data processing system, version 2016, https://www.njoy21.io/NJOY2016/

[68] J.-Ch. Sublet, L.W. Packer, J. Kopecky, R.A. Forrest, A.J. Koning, D.A. Rochman, The European Activation File: EAF-2010 neutron-induced cross section library, EASY Documentation Series CCFE-R (10) 05, 2010, http://www.ccfe.ac.uk/EASY-data/eaf2010/Docs/EAF_n_Cross_sections_2010.pdf

[69] K. Shibata, O. Iwamoto, T. Nakagawa, N. Iwamoto, A. Ichihara, S. Kunieda, S. Chiba, K. Furutaka, N. Otuka, T. Ohsawa, T. Murata, H. Matsunobu, A. Zukeran, S. Kamada, J. Katakura: JENDL-4.0: A new library for Nuclear Science and Engineering, *J. Nucl. Sci. Technol.* 48(1) (2011) 1, https://wwwndc.jaea.go.jp/jendl/j40/update/

[70] JENDL-4.0 High Energy File, https://wwwndc.jaea.go.jp/ftpnd/jendl/jendl40he.html

[71] JENDL Activation Cross Section File for Nuclear Decommissioning 2017 (JENDL/AD-2017), https://wwwndc.jaea.go.jp/ftpnd/jendl/jendl-ad-2017.html

[72] JENDL High Energy File 2007, https://wwwndc.jaea.go.jp/ftpnd/jendl/jendl-he-2007.html

[73] TALYS-based evaluated nuclear data library, TENDL-2017, https://tendl.web.psi.ch/tendl_2017/tendl2017.html

[74] The Joint Evaluated Fission and Fusion File. JEFF-3.3, http://www.oecd-nea.org/dbdata/jeff/jeff33/index.html

[75] S.F. Mughabghab, Atlas of neutron resonances, Elsevier, 2006.

[76] A.J. Koning, D. Rochman, J. Kopecky, J. Ch. Sublet, E. Bauge, S. Hilaire, P. Romain, B. Morillon, H. Duarte, S. van der Marck, S. Pomp, H. Sjostrand, R. Forrest, H. Henriksson, O. Cabellos, S. Goriely J. Leppanen, H. Leeb, A. Plompen, R. Mills, TENDL-2015: TALYS-based evaluated nuclear data library, https://tendl.web.psi.ch/tendl_2015/tendl2015.html

[77] V.S. Barashenkov, B.F. Kostenko, A.M. Zadorogny, Time-dependent intranuclear cascade model, *Nucl. Phys.,* A338 (1980) 413.

[78] V.S. Barashenkov, Monte Carlo simulation of ionization and nuclear processes initiated by hadron and ion beams in media, *Comp. Phys. Comm.,* 126 (2000) 28.

[79] S.G. Mashnik, A.J. Sierk, CEM03.03 user manual, Report LA-UR-12-01364, (2012).

[80] S.G. Mashnik, L.M. Kerby, MCNP6 simulation of light and medium nuclei fragmentation at intermediate energies, EPJ Web of Conferences, 117 (2016) 03008, https://doi.org/10.1051/epjconf/201611703008

[81] A.Yu. Konobeyev, U. Fischer, P.E. Pereslavtsev, S.P. Simakov, Status of the n+^{180,183}W evaluation, NEA OECD, EFFDOC-1386 (2019).

[82] P. Pereslavtsev, A. Konobeev, Nuclear data evaluation for n+^{184}W. "Tungsten reload“, NEA OECD, EFFDOC-1332 (2017), http://www.oecd-nea.org/dbdata/nds_effdoc/effdoc-1332.pdf

Appendix

I. The file "*W.loc*" with deformation parameters used for n+^{180}W calculations. The corresponding line in the TALYS input file is "*deformfile 74 W.loc*"

top of file
```
 74 180    5    R    B                                                    180W
   0    R    0             0.24500    -0.05600
   1    R    0
   2    R    0
   3    R    0
   7    R    0
```
end of file

II. Changes in Subroutine PROCESSCHANNELS of the TEFAL code [12] (in red)

```
      subroutine processchannels
<...>
      real    xsex,E0,Elast,ee,Eo(0:numen2),xso(0:numen2),ea,eb,y1,y2,
     +        xsint,specmass,xsy,tot,totE,Eaverage
c add 1 line:
      real  Eletzte,QQ
<...>
              Ehist(idc,nen,type,nenout)=0.5*(Eout(idc,nen,nenout-1)+
     +          Eout(idc,nen,nenout))*specmass
c add 6 lines:
          if(type==1.and.idc==1.and.nenout==nend0) then
          QQ=Qdisc(type,nlevmax)
          Eletzte=specmass* (eninc(nin)*specmass +QQ)
          If(Eletzte>0.0.and.Eletzte > Ehist(idc,nen,type,nenout))
     1             Ehist(idc,nen,type,nenout)=Eletzte
                                                  endif
  290       continue
<...>
```

KIT Scientific Working Papers
ISSN 2194-1629